



**Gustavo Nuno Martins Eduardo**

Licenciado

**Impact of chromosomal structure on the  
evolution of *Schizosaccharomyces  
pombe* undergoing Mutation  
Accumulation**

Dissertação para obtenção do Grau de Mestre em  
Genética Molecular e Biomedicina

Orientador: Lília Perfeito, PhD, Principal Investigator no  
Instituto Gulbenkian de Ciência.

Júri:

Presidente: Prof. Doutora Paula Gonçalves  
Arguente: Prof. Doutor Francisco Dionísio  
Vogal: Prof. Doutora Lília Perfeito

LOMBADA



FACULDADE DE  
CIÊNCIAS E TECNOLOGIA  
UNIVERSIDADE NOVA DE LISBOA

bro, 2015



Impact of chromosomal structure on the evolution of Schizosaccharomyces  
pombe undergoing Mutation Accumulation



FACULDADE DE  
CIÊNCIAS E TECNOLOGIA  
UNIVERSIDADE NOVA DE LISBOA



FUNDAÇÃO CALOUSTE GULBENKIAN  
Instituto Gulbenkian de Ciência

Department of Life Sciences, Faculty of Sciences and Technology, New University of Lisbon  
Evolution and Genome Structure Group, Instituto Gulbenkian de Ciência

Gustavo Nuno Martins Eduardo

**Impact of chromosomal structure on the evolution of  
*Schizosaccharomyces pombe* undergoing Mutation Accumulation**

Dissertation to obtain an MSc in Molecular Genetics and Biomedicine

Orientador: Lília Perfeito, Principal Investigator, Instituto Gulbenkian de Ciência

**October 2015**

Impact of chromosomal structure on the evolution of *Schizosaccharomyces pombe* undergoing Mutation Accumulation

Copyright Gustavo Nuno Martins Eduardo, FCT/UNL, UNL

A Faculdade de Ciências e Tecnologia e a Universidade Nova de Lisboa têm o direito, perpétuo e sem limites geográficos, de arquivar e publicar esta dissertação através de exemplares impressos reproduzidos em papel ou de forma digital, ou por qualquer outro meio conhecido ou que venha a ser inventado, e de a divulgar através de repositórios científicos e de admitir a sua cópia e distribuição com objectivos educacionais ou de investigação, não comerciais, desde que seja dado crédito ao autor e editor.

## ***Aknowledgements***

To my parents. Another step on the ladder.

I'd like give Lília Perfeito my most profound gratitude. I can't thank you enough for this opportunity. Thank you for all I've learned while working in the EGS group and for all the help you've given me during this past year.

This thank you extends to all the people I've worked with in my time here. Catarina, Diogo, Paula, Sara, Simone, this Thesis wouldn't have been done without you. I include here Isabel Gordo, for giving me ideas I would not have thought of otherwise. And, of course, to Teresa Avelar, who has never met me but without whose work mine would not have been possible. And I could not forget Rui Gardner, Cláudia and Cláudia, for all the help they gave me with the FACS technique.

I'd also like to thank Prof. Paula Gonçalves, for being understanding of my situation and helping me when I most needed it.

Thanks to all the MIGS, to Mauro and to Lucas for the support and for trying to keep me socially active.

Paul, Lukas, Zack, and Vince, thank you for keeping me sane.

# TABLE OF CONTENTS

Abbreviations.....	vii
Abstract.....	ix
Resumo.....	ix
Keywords.....	ix
1. Introduction.....	1
<b>1.1 State of the art and objectives</b> .....	<b>1</b>
<b>1.2 On <i>S. pombe</i></b> .....	<b>3</b>
<b>1.3 On our genomic alterations</b> .....	<b>4</b>
<b>1.4 Recombination and genetic interactions</b> .....	<b>5</b>
2. Materials and Methods.....	7
<b>2.1 Material, media and strains</b> .....	<b>7</b>
<b>2.2 Mutation Accumulation</b> .....	<b>9</b>
<b>2.3 Assessment of the number of cells picked during MA</b> .....	<b>10</b>
<b>2.4 Freezing and unfreezing samples</b> .....	<b>11</b>
<b>2.5 Fitness Assay</b> .....	<b>12</b>
<b>2.6 Statistical analysis and parameter estimation</b> .....	<b>15</b>
<b>2.7 Tetrad Dissection</b> .....	<b>16</b>
<b>2.8 Comparisons between fitness and genotype</b> .....	<b>18</b>
3. Results.....	19
<b>3.1 Assessment of the number of cells picked during mutation accumulation</b> .....	<b>19</b>
<b>3.2 Mutation accumulation and competitions</b> .....	<b>20</b>
<b>3.3 Mutation parameter estimation</b> .....	<b>28</b>
<b>3.4 Test for genetic interactions between a rearrangement and accumulated mutations</b> .....	<b>31</b>
<b>3.5 Comparisons between fitness and genotype</b> .....	<b>33</b>
4. Discussion.....	37
<b>4.1 Mutation accumulation</b> .....	<b>37</b>
<b>4.2 Fitness trajectories</b> .....	<b>37</b>
<b>4.3 Recombinant hybrids</b> .....	<b>39</b>
<b>4.4 Mutation parameters</b> .....	<b>41</b>
<b>4.5 Future Work</b> .....	<b>41</b>
5. Bibliography.....	43

<b>5.1 Journal references .....</b>	<b>43</b>
<b>5.2 Electronic references .....</b>	<b>45</b>
<b>6. Supplementary Materials .....</b>	<b>47</b>

# LIST OF FIGURES

Figure 1.1: Graphical representation of the chromosomes and chromosomal rearrangements present in the strains used during this project. .... 5

Figure 2.1 Example of YES agar plate used to streak each strain's 12 cell lines. The grid pattern allows us to streak all 12 on the same plate, one per area. .... 9

Figure 2.2 LSR Fortessa interface, showing an example of a well's cells being separated through the three windows and between the mCherry-marked reference competitor and the interest sample strain. .... 13

Figure 3.1: Probability of isolating one, two or three cells per bottleneck. The error bars represent standard deviation from the mean. The data represents the pooled results of three experiments, each analyzing 96 streaks ..... 19

Figure 3.2 Average fitness trajectories for strains SPP26 (in light blue) and SPP27 (in dark blue) across three different bottleneck numbers: B0, B48 and B144. For B0 the error bars represent experimental error from several measurements of the ancestral strain, while for B48 and B144 they represent the variance between all 12 cell lines per strain. \* shows a significant change in fitness distributions between both bottleneck numbers, while  $\Delta$  does the same for fitness average. \*/ $\Delta$  p-value < 0.05; \*\*/ $\Delta$   $\Delta$  p-value < 0.01; \*\*\*/ $\Delta$   $\Delta$   $\Delta$  p-value < 0.001. Bonferroni corrections were applied to all p-values. .... 21

Figure 3.3 Average fitness trajectories for strains C2 (blue) and I2 (red) across three different bottleneck numbers: B0, B48 and B144. For B0 the error bars represent experimental error from several measurements of the ancestral strain, while for B48 and B144 they represent the variance between all 12 cell lines per strain. \* shows a significant change in fitness distributions between both bottleneck numbers, while  $\Delta$  does the same for fitness average. \*/ $\Delta$  p-value < 0.05; \*\*/ $\Delta$   $\Delta$  p-value < 0.01; \*\*\*/ $\Delta$   $\Delta$   $\Delta$  p-value < 0.001. Bonferroni corrections were applied to all p-values. .... 22

Figure 3.4 Average fitness trajectories for strains C4 (blue) and T4 (red) across three different bottleneck numbers: B0, B48 and B144. For B0 the error bars represent experimental error from several measurements of the ancestral strain, while for B48 and B144 they represent the variance between all 12 cell lines per strain. \* shows a significant change in fitness distributions between both bottleneck numbers, while  $\Delta$  does the same for fitness average. \*/ $\Delta$  p-value < 0.05; \*\*/ $\Delta$   $\Delta$  p-value < 0.01; \*\*\*/ $\Delta$   $\Delta$   $\Delta$  p-value < 0.001. Bonferroni corrections were applied to all p-values. .... 23

Figure 3.5 Average fitness trajectories for strains C5 (blue), T5 (red) and SPP20 (pink) across three different bottleneck numbers: B0, B48 and B144 (not performed for SPP20 at this time). For B0 the error bars represent experimental error from several measurements of the ancestral strain, while for B48 and B144 they represent the variance between all 12 cell lines per strain. \* shows a significant change in fitness distributions between both bottleneck numbers, while  $\Delta$  does the same for fitness average. \*/ $\Delta$



p-value < 0.05; \*\*/ $\Delta$  p-value < 0.01; \*\*\*/ $\Delta \Delta$  p-value < 0.001. Bonferroni corrections were applied to all p-values. .... 24

Figure 3.6 Average fitness trajectories for strains C8 (blue) and T8 (red) across three different bottleneck numbers: B0, B48 and B144. For B0 the error bars represent experimental error from several measurements of the ancestral strain, while for B48 and B144 they represent the variance between all 12 cell lines per strain. \* shows a significant change in fitness distributions between both bottleneck numbers, while  $\Delta$  does the same for fitness average. \*/ $\Delta$  p-value < 0.05; \*\*/ $\Delta \Delta$  p-value < 0.01; \*\*\*/ $\Delta \Delta$  p-value < 0.001. Bonferroni corrections were applied to all p-values. .... 25

Figure 3.7 Average fitness trajectories for strains C10 (blue) and T10 (red) across three different bottleneck numbers: B0, B48 and B144. For B0 the error bars represent experimental error from several measurements of the ancestral strain, while for B48 and B144 they represent the variance between all 12 cell lines per strain. \* shows a significant change in fitness distributions between both bottleneck numbers, while  $\Delta$  does the same for fitness average. \*/ $\Delta$  p-value < 0.05; \*\*/ $\Delta \Delta$  p-value < 0.01; \*\*\*/ $\Delta \Delta$  p-value < 0.001. Bonferroni corrections were applied to all p-values. .... 26

Figure 3.8 Change in variance from B0 to B144 for each individual strain, with the exception of SPP20, which shows the difference in variance between B0 and B48. .... 27

Figure 3.9 Relationship between initial fitness (B0) and average fitness at B144. .... 30

Figure 3.10 Relationship between initial fitness (B0) and average fitness at B144 for strains SPP26, I2, C2, C4, T5, C5, T8, C8, T10 and C10..... 30

Figure 3.11 Distribution of fitness frequencies of 2 sets of hybrids: those resulting from a cross between ancestral C5 and ancestral C4 strains (green line); and those resulting from the cross between ancestral C5 and a C4 line that underwent 48 bottlenecks (purple line). .... 32

Figure 3.12 Distribution of fitness frequencies of two sets of hybrids: those resulting from a cross between ancestral C5 and ancestral T4 strains (green line); and those resulting from the cross between ancestral C5 and a T4B48 strain (purple line)..... 33

# LIST OF TABLES

Table 2.1 Strains used in this Thesis. ....	8
Table 3.1 Results from fitting the Analysis of Variance Model (ANOVA) comparing $\Delta W$ (fitness at B144 subtracted from fitness at B0) all lines from different genomic backgrounds. Red indicates p-value < 0.05, yellow indicates $0.01 > p\text{-value} > 0.001$ and green indicates $0.001 > p\text{-value}$ . Bonferroni corrections were applied to all p-values. ....	27
Table 3.2 Fitness decline per mutation, arising mutations per generation, associated errors and mean mutation per generation of each strain. ....	29
Table 3.3 Results of the fit of a 3-Way ANOVA correlating the presence of each auxotrophic marker in C5/C4.3 hybrid samples with those samples' fitness level as the dependent variable. * p-value < 0.05; ** p-value < 0.01; *** p-value < 0.001 ....	34
Table 3.4 Results of the fit of a 3-Way ANOVA correlating the presence of each auxotrophic marker in C5/T4.11 hybrid samples with those samples' fitness level as the dependent variable. * p-value < 0.05; ** p-value < 0.01; *** p-value < 0.001 ....	35
Table 6.1 C5+C4.3 and C5+T4.11 samples organized by tetrad the spore originated from and marked with parental or mixed phenotypes. ....	47
Table 6.2 Individual fitness values for all replicates of strain SPP26 and corresponding lines, across bottlenecks 0, 48 and 144. Blank cells represent replicates that could not be measured or were used as controls. ....	48
Table 6.3 Individual fitness values for all replicates of strain SPP27 and corresponding lines, across bottlenecks 0, 48 and 144. Blank cells represent replicates that could not be measured or were used as controls. ....	49
Table 6.4 Individual fitness values for all replicates of strain I2 and corresponding lines, across bottlenecks 0, 48 and 144. Blank cells represent replicates that could not be measured or were used as controls. ....	50
Table 6.5 Individual fitness values for all replicates of strain C2 and corresponding lines, across bottlenecks 0, 48 and 144. Blank cells represent replicates that could not be measured or were used as controls. ....	51
Table 6.6 Individual fitness values for all replicates of strain T4 and corresponding lines, across bottlenecks 0, 48 and 144. Blank cells represent replicates that could not be measured or were used as controls. ....	52
Table 6.7 Individual fitness values for all replicates of strain C4 and corresponding lines, across bottlenecks 0, 48 and 144. Blank cells represent replicates that could not be measured or were used as controls. ....	53

Table 6.8 Individual fitness values for all replicates of strain T5 and corresponding lines, across bottlenecks 0, 48 and 144. Blank cells represent replicates that could not be measured or were used as controls. ....	54
Table 6.9 Individual fitness values for all replicates of strain C5 and corresponding lines, across bottlenecks 0, 48 and 144. Blank cells represent replicates that could not be measured or were used as controls. ....	55
Table 6.10 Individual fitness values for all replicates of strain SPP20 and corresponding lines, across bottlenecks 0, 48 and 144. Blank cells represent replicates that could not be measured or were used as controls. ....	56
Table 6.11 Individual fitness values for all replicates of strain T8 and corresponding lines, across bottlenecks 0, 48 and 144. Blank cells represent replicates that could not be measured or were used as controls. ....	57
Table 6.12 Individual fitness values for all replicates of strain C8 and corresponding lines, across bottlenecks 0, 48 and 144. Blank cells represent replicates that could not be measured or were used as controls. ....	58
Table 6.13 Individual fitness values for all replicates of strain T10 and corresponding lines, across bottlenecks 0, 48 and 144. Blank cells represent replicates that could not be measured or were used as controls. ....	59
Table 6.14 Individual fitness values for all replicates of strain C10 and corresponding lines, across bottlenecks 0, 48 and 144. Blank cells represent replicates that could not be measured or were used as controls. ....	60
Table 6.15 Individual fitness values for all replicates of the recombinant hybrids .....	61

## Abbreviations

**96 Deep Well plate** – VWR 96-well deep well blocks

**96 small well plate** – Corning Incorporated COSTAR 96 Well Cell Culture Plates

**B0** – Ancestral cell line

**B48** – Cell line after 48 bottlenecks

**B144** – Cell line after 144 bottlenecks

**°C** – Degrees Celsius

**C** – Control strain

**FACS** – Fluorescence Activated Cell Sorting

**FM** – Freezing Medium

**I** – Strain carrying a chromosomal inversion

**KS test** – Kolmogorov-Smirnov test

**MA** – Mutation Accumulation

**MCMC** – Markov Chain Monte-Carlo

**mL** – Milliliters

**nm** – Nanometer

**PMG** – Pombe Glutamate Medium

**RPM** – Rotations Per Minute.

**T** – Strain carrying a chromosomal translocation

**Wilcox test** – Mann-Whitney-Wilcoxon test

**WT** – Wild Type strain

**YES** – Yeast Extract with Supplements

$U_d$  – Mean number of arising deleterious mutations per generation

$s_d$  – Fitness decline caused by each deleterious mutation (selection coefficient)

$\lambda(G)$  – Mean mutations present at generation G

$\delta s_d$  – Error associated with  $s_d$

$\delta U_d$  – Error associated with  $U_d$

$\Delta W$  – Change in fitness (fitness at bottleneck 144 subtracted from ancestral fitness)

$\mu L$  – Microliters

$\chi^2$  – Chi-square test

## Abstract

Large chromosomal rearrangements are common in natural populations and thought to be involved in speciation events. In this project, we used experimental evolution to determine how the speed of evolution and the type of accumulated mutations depend on the ancestral chromosomal structure and genotype. We utilized two Wild Type strains and a set of genetically engineered *Schizosaccharomyces pombe* strains, different solely in the presence of a certain type of chromosomal variant (inversions or translocations), along with respective controls. Previous research has shown that these chromosomal variants have different fitness levels in several environments, probably due to changes in the gene expression along the genome. These strains were propagated in the laboratory at very low population sizes, in which we expect natural selection to be less efficient at purging deleterious mutations. We then measured these strains' changes in fitness throughout this accumulation of deleterious mutations, comparing the evolutionary trajectories in the different rearrangements to understand if the chromosomal structure affected the speed of evolution. We also tested these mutations for possible epistatic effects and estimated their parameters: the number of arising deleterious mutations per generation ( $U_d$ ) and each one's mean effect ( $s_d$ ).

## Resumo

Grandes rearranjos cromossómicos são comuns em populações naturais e crê-se que estejam envolvidos em eventos de especiação. Neste projecto, usámos evolução experimental para determinar em que medida o ritmo da evolução e o tipo de mutações acumuladas dependem da estrutura cromossómica ancestral e do genótipo. Utilizámos duas estirpes Wild Type e um conjunto de estirpes de *Schizosaccharomyces pombe* geneticamente alteradas, juntamente com os respectivos controlos. Investigação prévia demonstrou que estas variantes cromossómicas apresentam diferentes níveis de fitness em vários ambientes, provavelmente devido a à alteração da expressão génica ao longo do genoma. Estas estirpes foram propagadas no laboratório com tamanhos populacionais diminutos, que nós expectamos que levem a selecção natural a não ser tão eficiente a eliminar mutações deletérias. Medimos as alterações de fitness destas estirpes ao longa da acumulação de mutações deletérias, comparando as trajectórias evolutivas dos diferentes rearranjos para entender se a estrutura cromossómica afecta o ritmo da evolução. Também testámos os possíveis efeitos epistáticos destas mutações e estimámos os seus parâmetros: o número de mutações deletérias que surgem por geração ( $U_d$ ) e o efeito médio de cada uma ( $s_d$ ).

**Keywords:** *Schizosaccharomyces pombe*; Chromosomal rearrangements; Mutation Accumulation; Recombination; Evolution

# 1. Introduction

---

## 1.1 State of the art and objectives

The study of evolution has come a long way since its inception. Our understanding of our biology and how life came to be was revolutionized with Darwin's ideas on the origins of species (Darwin 1859), which introduced terms such as evolution and natural selection into popular parlance. Darwin's discoveries spurred many doubts, and breached just as many taboos, on when and how Life itself had come to be (Dunwell, 2007). One concept that would later strengthen Darwin's hypothesis was the existence of genes. The study of heredity, and by consequence genetics, was first pioneered by Mendel in 1865 through the study of peas. Perhaps due to such humble beginnings, his discoveries would be forgotten for over three decades until de Vries and others once more found Mendel's manuscripts and published his findings. Despite that world-changing insight into the very nature of life itself, it would not be until 1906 that Bateson would try, on an address aimed at the Neurological Society of London, to convince the members of the Society to consider the importance the study of heredity and genetics had on the human condition (Bateson, 2009). With time, this fledgling area of Science grew in size and importance. In one century, the field of Genetics has grown from applied horticulture to a branch of Science that integrates plant, animal, microorganical, fungal and human research. With today's knowledge of DNA and RNA, epigenetics and inheritance, the study of genetics and evolution has proven its importance as a useful tool in the realms of not only horticulture, but also animal husbandry, oncology and pharmacology, among many others (Dunwell, 2007).

And yet, despite all of these advances, we still can't fully answer the question: How does evolution work? Evolutionary biologists have struggled for decades to provide a definitive answer. Although the general mechanisms through which evolution works are well known, including natural selection, random mutations and recombination, there are still many factors that cloud our understanding of this process so necessary for the existence of life on Earth. For example, what are the advantages and disadvantages of sexual reproduction when compared to asexuality (Morran *et al.*, 2009). Or what is the exact relationship between selection and mutation, the balance of which maintains standing genetic variance (Barton, 2010).

Since mutation is the ultimate source of all genetic variation (Barton, 2010), studies of the accumulation of deleterious mutations under controlled selection environments can shed light on several topics related to evolution and its workings (Chevin, 2011; Gordo & Dionisio, 2005)

With that in mind, we performed a *Mutation Accumulation* (MA) experiment. MA consists in reducing the population size and hence increasing the role of genetic drift in an evolving population. It leads to the random accumulation of mutations, independently of their effects on fitness. It was first pioneered

in *Drosophila melanogaster* (Bateman, 1959) and later adapted to different organisms, including *Saccharomyces cerevisiae* (Zeyl & DeVisser, 2001) and *Escherichia coli* (Kibota & Lynch, 1996). More recently, it was used in combination with whole genome sequencing to estimate the base substitution rate in *Schizosaccharomyces pombe* (Farlow et al., 2015).

MA experiments allow us to address whether different strains accumulate deleterious mutations at different rates or in different ways (in opposition, and complementation, of an adaptation experiment). In order to do that, first we must decrease selective pressure to its absolute minimum, so any mutation that's accumulated can be carried on to the descendants. Since we can only propagate survivors, this experimental design cannot capture lethal mutations.

*S. pombe* growing in asexual conditions propagates by binary fission, such that two sister cells are produced with the exact same genotype with the exception of new mutations. As they grow, they will naturally compete for space and nutrients present in their environment, so even if mutations have small effects, the one that allows its carrier cell to be fitter will be selected for. In an MA, we want to reduce this competition as much as possible. The way to do this is to isolate a single cell, so all of its descendants will carry its own accumulated mutations without competing with other, fitter genotypes. Such precautions, along with usual microbiological research staples such as growing the cells at optimal growth temperatures and consistently applying the same treatments to all our cultures, allow us to ensure the carry-over of mutations, even those with highly deleterious effects, over thousands of generations. We use rich media so all genotypes have the same advantage when it comes to gathering nutrients from the medium; for example, if a cell mutates in a way that it can no longer produce a certain aminoacid it needs, it will die in a medium without that aminoacid. Hence, the mutations responsible for that inability to produce the aminoacid will be selected against.

Unlike previous studies, we performed this experiment using strain with several chromosomal rearrangements of *Schizosaccharomyces pombe* (*S. pombe*). It has been estimated that three quarters of all species of *Drosophila* are polymorphic for inversions, and chromosomal rearrangements are common in natural isolates of *S. pombe*. It might be the case that chromosomal rearrangements contribute to the processes of speciation and adaptation (Avelar, 2012). If so, then we expect different chromosomal rearrangements to take different trajectories throughout their evolution, even if the same genetic material is present in all of them. The fact that the genome has been reorganized may lead to the appearance of different mutations, or similar mutations that have differing effects.

In another area of investigation, the dynamics between epistasis and evolution still pose several questions which are not fully understood (de Visser *et al.*, 2011). Epistasis is a phenomenon whereby the combined effect of two mutations is different from simply adding the effects of the mutations in isolation. Since an MA produces lines with large numbers of mutations, it is an ideal raw material to study epistasis. For that effect, we crossed mutated strains with a non-mutated background. In order to



control for genetic background effects, we also crossed non-mutated versions of those same strains with the same non-mutated background. As such, the difference between the recombinant spores produced from those crosses should be exclusively due to the presence of the accumulated mutations.

To analyze these crosses we dissected the tetrads formed from each cross, separating their individual recombinant spores. This technique gives us great statistic power, as it allows us to peer into what's happening within each of the four spores each tetrad carries, instead of averaging out their genotypes.

In short, we began this work with the intention to answer three main questions:

1. Will chromosomal rearrangements alter the accumulation of mutations and/or their effects?
2. Are the accumulated mutations epistatic in effect?
3. How do our strains' mutation parameters compare to those estimated for other species?

## **1.2 On *S. pombe***

*S. pombe* was the model organism chosen for our work due to, firstly, the common advantages it shares with other microbiological models, such as that it is easy to grow and store in large numbers. It is also easy to genetically manipulate, useful traits when studying adaptation and evolution (Avelar *et al.*, 2013). We have extensive knowledge of its biology, particularly when it comes to chromosome maintenance. It is therefore an ideal model to study the interplay between genome architecture and evolution.

*S. pombe* is also preferentially haploid; in a study done by Brown *et al.*, out of 81 natural isolate and 3 laboratory strains, only 1 was diploid (Brown *et al.*, 2011). The strains we use in our lab are all haploid as well, entering a temporary state of diploidy only if reproducing sexually (Avelar, 2012). Haploidy ensures that any given mutation's effect on phenotype will be expressed without any homologous alleles to mask its expression.

Being an eukaryotic organism, the findings on *S. pombe* might later be applicable to other eukaryotic genomes, including humans. Its genome has also been fully sequenced. Most of these characteristics are shared by other organisms, such as *Saccharomyces cerevisiae*. We chose to study *S. pombe* for its lower number of chromosomes, which are larger in size than in *S. cerevisiae*. In such a genome, there are less possible combinations of chromosomal rearrangements and each has a bigger effect, since it affects more genes. It also has the distinction of being the eukaryote with the lowest number of genes, lower even than some prokaryotes (Yanagida, 2002).

### 1.3 On our genomic alterations

Besides strains carrying chromosomal rearrangements and their respective controls, we also used two Wild Type-like strains in our experiments, SPP26 and SPP27, which were isolated from a natural strain and propagated in labs before being donated to our collection. SPP26 was donated to us from the Portuguese Yeast Culture Collection at Faculdade de Ciências e Tecnologia (FCT) by Dr. José Paulo Sampaio. SPP27 was descended from Urs Leopold's original natural isolates and was donated to us by the I. Tolic in Gottingen, Germany.

For our chromosomal rearrangement-carrying strains, we used those engineered by Teresa Avelar during her PhD Thesis Project "Chromosomal structure: a selectable trait for evolution". We used 10 strains engineered by her: 5 rearrangements (4 translocations and 1 inversion) and 5 controls. *Inversion 2* (I2) is an inversion in chromosome 2, between the sites of the *arg7* and *lys4* genes. *Translocation 4* (T4) has translocated parts of the long arms of chromosomes 2 and 3. Translocation 5 has translocated parts of the short arm of chromosome 1 and the long arm of chromosome 2. *Translocation 8* (T8) has translocated parts of the short arm of chromosome 2 and the long arm of chromosome 3. *Translocation 10* (T10) has translocated parts of the short arm of chromosome 1 and the long arm of chromosome 3. These were created using the Cre-loxP system, in which a gene disruption cassette is flanked by loxP sites (Avelar, 2012). The insertion of these loxP cassettes in specific locations of the chromosomes allows chromosomal breakage and following recombination between those locations (Avelar, 2012; Carter & Delneri, 2010). Each of these rearrangements has a corresponding control strain: Inversion 2 corresponds to *Control 2* (C2), Translocation 4 to *Control 4* (C4), etc. These control strains carry the same genotype as the parental strain, except for with the addition of the loxP cassettes in the same locations as its respective rearrangement strain, which are inserted without causing the subsequent breakage and chromosomal rearrangement. Graphical representations of their chromosomes can be seen in Figure 1.1.

All strains used in this project were of the h<sup>-</sup> mating type with the exception of C5, which is h<sup>+</sup>. Later on in the experiment we added another strain, SPP20, which is an h<sup>-</sup> variation of C5, to control for this fact.

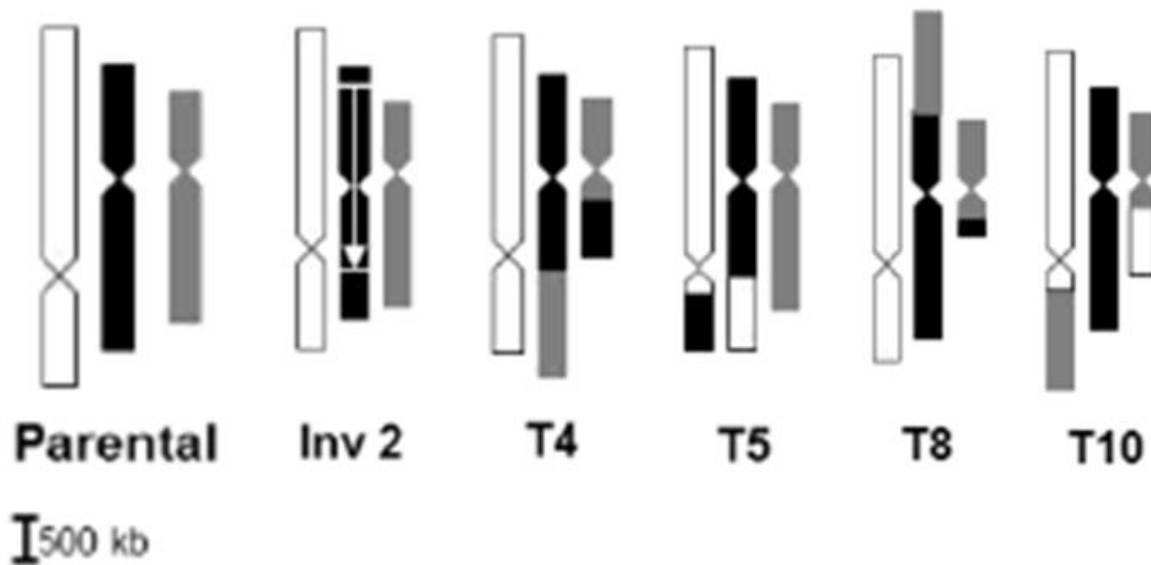


**Figure 1.1: Graphical representation of the chromosomes and chromosomal rearrangements present in the strains used during this project. The different colors indicate the parental chromosome of origin of each DNA stretch. The arrow shows an inversion. Figure adapted from Avelar 2013.**

As such, all chromosomal rearrangements and all their respective controls have the same genetic material, with the exception of their auxotrophic markers. The only difference between them is the organization of this material within the genome.

#### **1.4 Recombination and genetic interactions**

Using *S. pombe* as a model organism has one distinct advantage: we can control its sexual and asexual reproductive cycles. Most *S. pombe* grown in laboratories throughout the world have two mating types, h<sup>+</sup> and h<sup>-</sup>. One mating type can only sexually reproduce with the other, never with its own mating type. A cell's mating type is determined by the allele present in the *mat1* locus: *mat1-P* for h<sup>+</sup> and *mat1-M* for h<sup>-</sup>. In the wild, *S. pombe* actually tends to be of the h<sup>0</sup> mating type. These are cells that can freely interchange between the two mating types (so called because 90% of the cells in a culture are capable of switching). These are converted to either h<sup>+</sup> or h<sup>-</sup> cells through the silencing of the opposite mating type's gene (Forsburg & Rhind, 2006).

As stated before, with the exception of strain C5, all strains used in this project were of the h<sup>-</sup> mating type.

Merely being in the presence of the opposite mating type is not enough for sexual reproduction to occur. If in rich medium, *S. pombe* will opt to reproduce asexually, for maximum daughter-cell production. If

starved of nitrogen, however, it will instead opt to produce meiotic spores (Forsburg & Rhind, 2006). This allows us to choose when and what strains will reproduce sexually, and allows us to keep all others reproducing asexually throughout our experiments.

## 2. Materials and Methods

---

### 2.1 Material, media and strains

We grew *S. pombe* in three different media, depending on the experiment. As rich medium we used *Yeast Extract plus Supplements* (YES) medium, in both solid and liquid forms. Liquid YES is composed of Yes Extract and glucose, supplemented with adenine, histidine, leucine, uracil and lysine. Solid plates are made with YES agar, which follows the same recipe with the addition of 20g/L agar. As minimal medium we used Pombe Glutamate Medium (PMG), composed of potassium hydrogen phthalate,  $\text{Na}_2\text{HPO}_4$  and supplemented with salt, mineral and vitamin stocks. PMG without a carbon source was used to incubate cells in order to increase expression of the fluorescent protein mCherry. This medium allows us to keep *S. pombe* alive in solution for up to 48 hours at 4°C with no change in cellular frequencies, either by growth or by cell death. Strains were crossed on Malt Extract medium (mating medium), composed of Bacto-malt extract supplemented with arginine and lysine. Selective media were based on PMG-Glucose agar, adapting the recipe for the removal of one aminoacid at a time for each. All recipes were adapted from “Basic methods for fission yeast”(Forsburg & Rhind, 2006):

All pipetting, streaking and unfreezing procedures were done in sterile conditions using a Bunsen burner. To aid in avoiding possible bacterial contaminations, all media was supplemented with 0.1 µg/mL ampicillin.

Liquid cultures were grown in VWR 96-well deep well blocks (from here on out referred to as 96 Deep Well plate). These plates can hold up to 2 mL of volume. The high number of wells allows us to grow several strains at once or to do a high number of replicates for each experiment, as well as allowing us to discount wells for blanks and controls and still keep most wells producing data for later analysis.

Corning Incorporated COSTAR 96 Well Cell Culture Plates (from here on out referred to as 96 small well plate) can carry up to 200µL of volume and they were used for two purposes: to hold samples to be frozen at -80°C, their small size allowing us to store a large number of samples in a limited space; and for samples to be read in LSR Fortessa equipment, as mentioned on pages 20 and 21. The high number of wells gives us the same advantages mentioned for 96 Deep Well plates, and since both types of plate have the same number of wells, it is easy to pipette samples from one type of plate to the corresponding well on the other type, so we are sure of what’s in each well throughout a whole experiment.

The strains used in this Thesis had previously been created and described in “Chromosomal structure: a selectable trait for evolution” (Avelar, 2012), and are described in Table 2.1.

**Table 2.1 Strains used in this Thesis.**

Code	Genotype	Common name	Creator
SPP26	<i>PYCC 4197 matM:nat</i>	Wild Type	PYCC4197
SPP27	<i>L972 matM:nat</i>	Wild Type	L972
C2	<i>h- arg7::padh1-loxP- kanMX6R lys4::loxP-ura4- kanMX6R mat1-M::mat1-M-natMX6 leu1-32 ade6-M216 ura4+</i>	Control 2	Teresa Avelar
I2	<i>h- arg7::loxP- kanMX6R lys4:: padh1-loxP- ura4+ - kanMX6R mat1-M::mat1-M-natMX6 leu1-32 ade6-M216 ura4-D18</i>	Inversion 2	Teresa Avelar
C4	<i>h- arg1::padh1-loxP- kanMX6R lys4::loxP-ura4-k kanMX6R mat1-M::mat1-M-natMX6 leu1-32 ade6-M210</i>	Control 4	Teresa Avelar
T4	<i>h- arg1::loxP- kanMX6R lys4::padh1-loxP- ura4+ - kanMX6R mat1-M::mat1-M-natMX6 leu1-32 ade6-M210 ura4-D18 matM- natMX6R</i>	Translocation 4	Teresa Avelar
C5	<i>his1::loxP- kanMX6R lys4::padh1-loxP- ura4- kanMX6R mat1-M::mat1-P-natMX6 leu1-32 ade6-M210 ura4+ matM</i>	Control 5 h(+)	Teresa Avelar
SPP20	<i>h- his1::loxP- kanMX6R lys4::padh1-loxP-ura4- kanMX6R mat1-M::mat1-M-natMX6 leu1-32 ade6-M210 ura4+ matM</i>	Control 5 (h-)	Simone Delgado
T5	<i>h- his1::loxP- kanMX6R lys4::padh1-loxP- ura4+ - kanMX6R mat1-M::mat1-M-natMX6 leu1-32 ade6-M210 ura4-D18 matM</i>	Translocation 5	Teresa Avelar
C8	<i>h- arg1::padh1-loxP- kanMX6R arg7::loxP-ura4- kanMX6R mat1-M::mat1-M-natMX6 leu1-32 ade6-M210 ura4+ matM- natMX6R</i>	Control 8	Teresa Avelar
T8	<i>h- arg1:: loxP- kanMX6R arg7:: padh1-loxP- ura4+ - kanMX6R mat1-M::mat1-M-natMX6 leu1-32 ade6-M210 ura4-D18</i>	Translocation 8	Teresa Avelar
C10	<i>h- arg1::padh1-loxP- kanMX6R his1::loxP-ura4- kanMX6R mat1-M::mat1-M-natMX6 leu1-32 ade6-M210 ura4+ matM- natMX6R</i>	Control 10	Teresa Avelar
T10	<i>h- arg1::loxP- KanMX6R his1::padh1-loxP-ura4-kanMX6R mat1-M::mat1-M-natMX6 leu1-32 ade6-M210 ura4-D18</i>	Translocation 10	Teresa Avelar

## 2.2 Mutation Accumulation

At the beginning of the experiment all 12 strains were streaked on agar plates, which were left to grow at 32°C for 48 hours. After this time, 12 isolated colonies from each strain were picked to undergo *Mutation Accumulation* (MA). These were again streaked on new agar plates in order to pick isolated colonies once more, in a process of bottlenecking. (Trindade, Perfeito, & Gordo, 2010) An example of these agar plates can be seen in Figure 2.1. All 12 lines for each strain underwent this bottlenecking every 48 hours and were frozen every 12 bottleneckings.

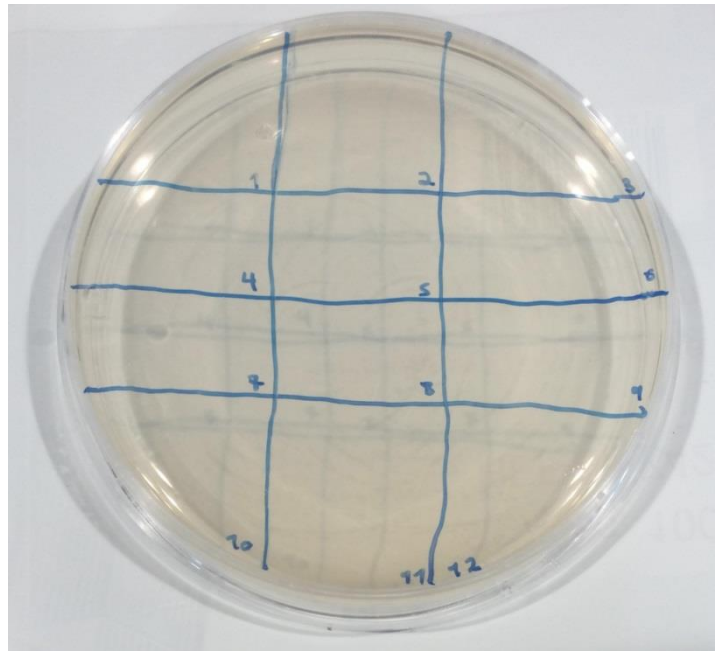


**Figure 2.1 Example of YES agar plate used to streak each strain's 12 cell lines. The grid pattern allows us to streak all 12 on the same plate, one per area.**

The number of generations that occur per bottleneck were estimated during previous experiments at the lab by counting the number of Colony Forming Units present in a colony after the usual 48 hours of growth ( $N_f$ ). Assuming each colony originates from a single cell, the number of generations elapsed will equal  $\log_2(N_f)$ . These calculations estimate each bottleneck corresponds to 16 generations, which means after 48 bottlenecks 768 generations have elapsed and 144 bottlenecks equal 2304 generations (A. P. Marques, personal communication).

C2, along with C8, are the only strains not to have 12 lines past bottleneck 48 (B48). Whenever a streaked colony fails to produce growth during a bottleneck, we go back to the previous bottleneck's plate and collect a new isolated colony, in order to recover the line and keep all 12 lines for each strain accumulating mutations throughout all bottlenecks. If the new colony is also unable to grow during the

next 48 hours, we once again go back to pick up yet a third isolated colony. However, if this happens a third time, we consider that line to have gone extinct, i.e., that the deleterious mutations it has accumulated have reached the threshold of lethality and will not allow viable daughter cells to replicate. We perform this recovery three times to ensure that the line is really lost due to deleterious mutations and not to a technical problem. We take note of which line went extinct and proceed with the experiment for the remaining ones. In this case, line C2.12 went extinct at bottleneck 132, so it is not represented in the data for bottleneck 144 (B144) competitions.

The MA propagation was carried out by myself and two other members of the lab: Simone Delgado and Paula Marques.

### **2.3 Assessment of the number of cells picked during MA**

An MA experiment is aimed at reducing selection as much as possible in order for mutations to accumulate close to the rate at which they appear. In microorganisms, this involves isolating single colonies and re-streaking them. Ideally each colony is the result of the growth of a single cell. To test whether this was the case in our experiment, we devised a protocol to assess the probability of carrying, and streaking, colonies which had grown from one single cell.

Three different *S. pombe* strains were grown from -80°C stocks, all variants of C4 of the same mating type and with different fluorescence markings: one marked with mCherry (the same used as the reference for competitions), one with GFP and the last unmarked (the same used in the MA experiment). These were grown on YES agar for 48 hours at 32°C, after which a piece of growth from each was placed in 5mL liquid YES and grown in a shaker at 32°C for 48 hours once more. From those cultures, which were presumably at similar concentration levels, 100µL of each were pipetted into an Eppendorf tube and mixed through up-and-down. Then, 5µL pipette tips were dipped in this solution and then simply touched upon a plate of YES agar. This size was chosen to produce a small droplet that gave rise to colonies close in size to the ones obtained during Mutation Accumulation experiment. The MA experiment was carried out by three different people in the lab and so we tested the streaking technique for every user. 96 such colonies were made for each one, to test all three individual techniques. We replicated the movements we used for each bottleneck: divided a YES agar plate into 12 sections and picked material from one mixed colony, streaking it inside one section.

Although they had come from mixed cultures, by streaking each colony we expected to isolate single cells. After another cycle of growth at 32°C for 48 hours we picked one colony from each section and streaked it once more onto new YES agar plates. If the streaking isolated single cells, then the resulting growth would present only one fluorescent marking per section; if not, then we would distinguish two



or three different colors in each. One final cycle of growth later, the plates were observed under the UV light of a Zeiss Stereo Lumar microscope. We then counted how many sections had only red growth, only green, only grey (not marked) growth, a mix of two colors or a mix of all three.

While calculating the odds of carrying a certain number of cells, we also had to take into account the possibility of carrying two or more cells with the same fluorescence. For example, a completely red colony might have grown from only one mCherry-marked cell, or it might also have grown from two or more mCherry-marked cells. A green and red colony must have been originated by at least one mCherry and one GFP-marked cells, or it could also have been formed from two or more mCherry-marked and one GFP-marked cells, two or more GFP-marked and one mCherry-marked cells or even multiple cells from each fluorescence type.

Due to the complexity of this estimation, we decided to use a *Markov Chain Monte-Carlo* (MCMC) algorithm to calculate the most likely probabilities for carrying any number of cells. This algorithm allows us to approximate an unknown probability distribution of our system at steady-state. By chaining together known probabilities starting from a known initial state, a trajectory to a final state can be simulated. Simulating many trajectories and many final states, and averaging the results, allows us to estimate the unknown probability distribution for the steady-state of our system (Fonnesbeck, 2014). This analysis was performed with the help of PhD student Diogo Santos.

As we perform MA on round plates, the grids we streak colonies in have rounded corners (Figure 2.1). We wanted to test whether the smaller streaking area would lead to a higher number of mixed colonies. We performed a  $\chi^2$  test to verify whether the number of mixed colonies in these corners was significantly higher than that of the other area of the grid.

## **2.4 Freezing and unfreezing samples**

We froze a sample of each cell line every 12 bottlenecks, to have material for competition assays and to serve as backup, or “fossil record”.

In order to freeze the samples, the first pipette tip used to make the first streak in the agar during MA was dipped into 500 $\mu$ L of liquid YES in a 96 Deep Well plate. These plates were then grown in a shaker at 32°C for 48 hours. Afterwards, the plates were centrifuged at 3500 RPM for 5 minutes, so as to conserve the maximum amount of cells when freezing. The supernatant was removed and the pellets resuspended in 150  $\mu$ L *Freezing Medium* (FM), a 1:1 mix of liquid YES with a 50% glycerol solution. The resulting suspension was pipetted into a 96 well plate, pre-cooled on dry ice, and then stored at -80°C.

When samples were needed, the 96 small well plates holding frozen samples were carried outside of the -80°C freezer while being kept on dry ice, so as to have the cells at room temperature for as little time as possible, as glycerol is toxic above freezing temperatures. Samples were taken from 48 wells at a time with the help of a replicator, whose tips had previously been sterilized by being dipped in pure alcohol, brought to a flame, and allowed to cool down before being inserted into the wells and then, carrying a droplet of the frozen samples of each tip, touched upon the surface of a YES agar plate.

After that, the 96 small well plate was returned to its place in the -80°C freezer as quickly as possible and the agar plates were placed at 32°C for 48 hours.

## 2.5 Fitness Assay

All fitness measurements were performed by competing test strains against a reference. All competitions assays were started from frozen samples, so as to keep consistency across all experiments. We measured competitive fitness for the ancestral strains (pre-MA), as well as all lines from bottlenecks 48 and 144 (B0, B48 and B144, respectively).

Every sample was competed against a reference strain marked with mCherry fluorescent marker. Both the competing cell lines and the reference strain were grown on YES agar plates at 32°C for 48 hours. Then a bit of growth was placed in a well in a 96 Depp Well plate containing 500µL liquid YES, whereupon they were placed once more at 32°C in a shaker for 24 hours. These wells were well mixed by pipetting before having their contents mixed in a well containing 180µL PMG in a 96 small well plate. Each well received 10µL of the reference strain and 10µL of the competing line. Though this 50/50 mix was the general case, some lines demanded different mix ratios, as explain in the next page. From this mixture, 20µL were placed in 500µL liquid YES in the corresponding well of a new 96 Deep Well plate, which went on to grow in a shaker at 32°C for 24 hours. The remaining 180µL were used to estimate cell numbers by FACS, following incubation for at least 2 hours in PMG This measurement was the first timepoint of the competition. Every day, during 7 days the cells were diluted in PMG and transferred to a new deep-well plate and placed at 32C. Hence, for each competition, we have 8 different time points.

The measurements were performed through *Fluorescence Activated Cell Sorting* (FACS) with LSR Fortessa equipment. This device is customizable with up to four lasers with modulable wavelengths and offers excellent sensibility and resolution (Becton *et al.*, 2011), making it ideal to measure small particles such as yeast cells. The software is easy to use and calibrate, and the machine itself quickens our research, as it can automatically reads complete 96 small well plates. Moreover, this method allows us to analyze 10 000 cells in less than 1 minute, giving us a strong statistical confidence.

We used two different lasers and wave-length receptors: one optimized for GFP and the other for mCherry. GFP was detected with a 488nm laser using a 530/30 nm bandpass filter, while mCherry was detected with a 561 nm laser using a 630/30 nm bandpass filter. The equipment was calibrated, with bi-weekly adjustments performed during maintenance, by the IGC Flow Cytometry Unit.

On the software's interface we define three windows (Figure 2.2), each with a gate to select cells of interest: the first to separate viable yeast cells from contaminations and cell debris; a second to separate singlets from cell aggregates; and a third to separate mCherry-marked cells from unmarked ones. This gave us a ratio, and a percentage, of how many unmarked cells there are, comparatively to the number of mCherry cells, there are in the mixture at each timepoint. If this number steadily increases across timepoints, it means the line's fitness is superior to the reference's; if it decreases, it means it's inferior.

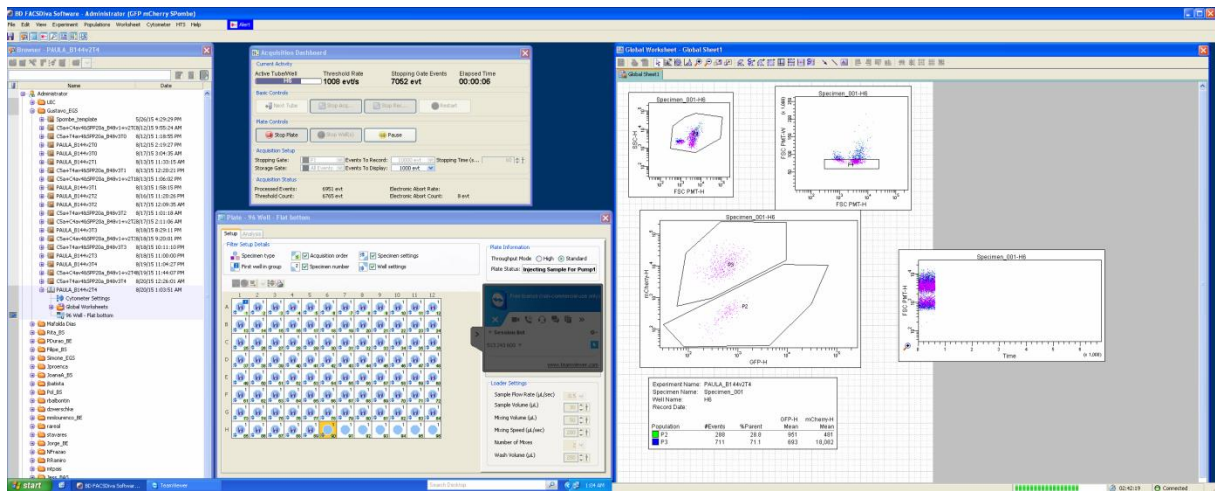


**Figure 2.2** LSR Fortessa interface, showing an example of a well's cells being separated through the three windows and between the mCherry-marked reference competitor and the interest sample strain.

Mixtures that reached mcherry frequencies higher than 99% or lower than 1% within few timepoints were not used in the experiment. This threshold was chosen because pure cultures of either mCherry or unmarked cells had around 1% of cells in the other gate. We used only those competitions that went through at least 3 timepoints before reaching those frequencies. For that effect, the replicate was repeated with different initial ratios of cells, adding less of the fittest competitor and more of the least fit (always in a total of 20μL) so as to delay one strain's dominance over the other.

The change in ratio of unmarked/mCherry cells across timepoints was then used to estimate fitness levels. If we assume exponential growth, then:

$$\text{Equation 1} \quad N(t) = N(0) * W^t$$

where  $N(t)$  is the number of cells at time  $t$  and  $W$  is the fitness of those cells. This equation can also be written as

$$\text{Equation 2} \quad W^t = \frac{N(t)}{N(0)}$$

We define relative fitness as

$$\text{Equation 3} \quad W_R = \frac{W_m}{W_{WT}}$$

where  $W_R$  is the relative fitness of the unmarked ( $m$ ) strain when compared to the reference strain ( $WT$ ), then by combining equations 1 and 2 we have

$$\text{Equation 4} \quad W_R^t = \frac{\frac{N_m(t)}{N_m(0)}}{\frac{N_{WT}(t)}{N_{WT}(0)}}$$

or, simplifying

$$\text{Equation 5} \quad W_R^t = \frac{N_m(t) * N_{WT}(0)}{N_m(0) * N_{WT}(t)}$$

We can take into account that the proportion of one type of cell is inversely proportional to the amount of its competitor present in the environment, and that the sum of both strains will equal 100% of the cells present in the environment. Ergo, if we define  $p(t)$  as the frequency of unmarked cells at time  $t$  and  $1-p(t)$  as the frequency of reference mCherry cells, we have

$$\text{Equation 3} \quad W_R^t = \frac{p(t)[1-p(0)]}{p(0)[1-p(t)]}$$

These calculations revolve around the curve measuring the percentage of each type of cells, marked and unmarked, in the medium. If we linearize this curve, we can directly correlate its slope with the relative fitness of the strains.

$$\text{Equation 4} \quad \ln(W_R^t) = \ln\left(\frac{p(t)[1-p(0)]}{p(0)[1-p(t)]}\right)$$

Defining the selection coefficient,  $s$ , as

$$\text{Equation 5} \quad s = \frac{\ln W_R^t}{t}$$

from equation 4 we get

$$\text{Equation 6} \quad st - \ln \frac{1-p(0)}{p(0)} = \ln \frac{p(t)}{1-p(t)}$$

Equation 5 defines a linear relationship between the natural logarithm of the ratio of frequencies and time (measured as number of generations for the reference, 8 per timepoint). By performing least squares linear regression we can estimate the slope of this line which gives us  $s$ . We can then estimate fitness using equation 4.

The mCherry reference strain has a fitness of 1 by definition, and the fitness values of all lines can be read as a comparison of that line's ability to survive and thrive in liquid YES when compared with the reference's own. For example, C4B0 possesses the fitness level closest to one, at  $0.992 \pm 0.003$ , apropos of being the most similar to the competing reference strain, which is a variation of C4 with the added mCherry fluorescent marker.

It should be noted that SPP20B0 fitness values had been measured during previous experiments at the laboratory, before the beginning of this Thesis' work, using the same methods used for all other strains.

## 2.6 Statistical analysis and parameter estimation

Between those bottlenecks whose lines' distribution of fitness values followed a Normal distribution, the data could be analyzed with Welch's T-test. To compare non-Normal datasets, or Normal datasets with not-Normal ones, we used the Kolmogorov-Smirnov's (KS) test. However, considering all bottleneck levels, including the ancestrals, had at least one not-Normal distribution, KS test was used to compare the distributions of all data pairs, to keep consistency across all analyses. KS test, as a non-parametric test, is also more conservative than T-test, giving us a greater certainty that the differences we find are actually significant.

Due to the fact that the median of each strain's fitness distribution changes throughout the experiment, and not just the distribution's shape and spread, we decided to also perform a test more sensitive to this last parameter. The significance of this value was calculated through the Mann-Whitney-Wilcoxon (Wilcox) Test. This way, we are sure the change is one of variance and of the average of all 12 lines' fitnesses.

Bonferroni corrections were applied by multiplying the p-value by the number of tests performed.

Using fitness data, we estimated the mutation parameters for each strain: the average fitness decline caused by each deleterious mutation ( $s_d$ ), the mean number of arising deleterious mutations per generation ( $U_d$ ) and the mean number of mutations ( $\lambda(G)$ ) present at each generation ( $G$ ). This was accomplished using the same methods as in Trindade *et al.* to estimate mutation parameters in *Escherichia coli* (Trindade *et al.*, 2010; Gordo & Dionisio, 2005; Colato & Fontanari, 2001):

$$\lambda(G) = \frac{U_d}{s_d} (1 - (1 - s_d)^G)$$

And  $s_d$  and  $U_d$  can be calculated through  $s_d = \frac{m_2}{m_1}$  and  $U_d = \frac{m_1}{(1-(1-s_d)^G)}$

where  $m_1$  is the slope of the natural logarithm of the mean fitness of all lines with bottleneck number and  $m_2$  is the slope of the natural logarithm of  $F_i$  with bottleneck number  $i$ .  $F_i$  can be calculated with the formula

$$F_i = \frac{\overline{W_i^2}}{\overline{W_i^2}}$$

$W$  corresponding to the mean fitness of each individual line at bottleneck  $i$ .

This model assumes no beneficial or compensatory mutations arise, only deleterious mutations, each with a selection coefficient  $s_d$ . Knowing the slopes  $m_1$  and  $m_2$  and their respective standard error ( $\delta$ ), one can estimate associated errors for  $U_d$  and  $s_d$ , calculated through error propagation as

$$\delta s_d = \left| \frac{\partial s_d}{\partial m_1} \delta m_1 \right| + \left| \frac{\partial s_d}{\partial m_2} \delta m_2 \right|$$

and

$$\delta U_d = \left| \frac{\partial U_d}{\partial s_d} \delta s_d \right| + \left| \frac{\partial U_d}{\partial m_1} \delta m_1 \right|$$

In order to test which backgrounds behave differently from each other, we fitted an Analysis of Variance Model (ANOVA) to check how the change in fitness (fitness at B0 subtracted from fitness at B144) correlated with each individual background.

All analysis were performed in Microsoft Excel or R Studio.

Mutation parameters could not be estimated for strain SPP20, for which only two of its bottlenecks' fitness levels were measured; to perform adequate calculations, at least three data points are necessary. The formulas used were also not applicable to strains C2 and T4 because these strains show strong signs of accumulation of beneficial mutations.

## 2.7 Tetrad Dissection

In order to test whether the mutations accumulated during the experiment were epistatic, i.e., whether they interacted, we crossed two evolved lines with an ancestral. This allowed us to separate the

accumulated mutations and directly test whether their effects were epistatic or additive. For that effect, we chose mutated lines from strains T4 (namely, T4.11) and C4 (namely, C4.3) from bottleneck 48. T4.11 was chosen due to its apparent beneficial mutations, and C4.3 was the most divergent C4 line at bottleneck 48 and hence the most likely to have accumulated mutations. These had to be crossed with an unmutated background, i.e. one at bottleneck 0, and the only strain used in this experiment of the opposite mating type was C5. We will call these two crosses C5/C4.3 hybrids and C5/T4.11 hybrids.

However, we needed to control for possible epistatic effects in the ancestral backgrounds. As such, we repeated the experiment with just unmutated strains. We crossed the same ancestral C5B0 with ancestral C4B0 and separately with T4B0. These crosses will be referred to as C5a/C4a hybrids and C5a/T4a hybrids, respectively.

As for the mating process itself, in order to mate, *S. pombe* haploids must be starved of nutrients (Nurse, 2000) specifically nitrogen (Forsburg & Rhind, 2006), or they will opt for asexual reproduction. For that effect, we unfreeze and take a bit of cellular growth of the strains we want to cross, grown in YES agar, and place it in 100 $\mu$ L PMG. We do a short centrifugation (1 minute at 3000 RPM) to form a pellet and take pipette the supernatant out. This process will clean the cells of nutrients they'd carry from the YES agar and is necessary for mating to occur. However, our strains tend to produce few spores, so we needed to increase the efficiency of the process. In order to do so, we starved our cells further. We did so by resuspending the pellet in a fresh 100 $\mu$ L PMG and letting it settle for half-an-hour/one hour,

This process leads the cells to consume their internal supplies of nutrients and to excrete their waste into the medium, which we remove. As such, they will go onward to be deposited onto the mating medium with no resources that would stimulate them to replicate instead of mate.

Once all cell samples were properly starved we mix resuspend them by up-and-down before pipetting 10 $\mu$ L of each into a new Eppendorf tube, where we mix the two we want to cross before pipetting 10 $\mu$ L of this mix onto mating medium. The droplets are allowed to dry by the flame before the plate is closed and sealed with parafilm and placed at 25°C for 48 hours. After these have passed, we take the plate out and take a bit of the colonies formed, one per mixture, to check under the microscope whether they've formed tetrads.

If successful, we suspend a portion of the growth on  $\approx$ 30 $\mu$ L PMG and pipette it onto a YES agar plate, which we tilt to form a line dividing the plate in two. It is on this plate that we dissect the tetrads, using Singer's MSM 400 Manual Dissection Microscope and following Paul Nurse's Fission Yeast Handbook's instructions (Nurse, 2000). Once the tetrads are dissected, we leave the plate growing at 32°C for 48 hours, upon which we'll have isolated colonies, each descended from a single spore.

These colonies were frozen using the same methods as those derived from MA, with the only difference being that the whole colony was put into liquid YES to grow. These frozen samples were also competed according to the methods described previously for MA samples.

## **2.8 Comparisons between fitness and genotype**

Just as two parental genomes are combining and interacting to form new distributions of fitness effects, this recombination can be seen in certain phenotypic characteristics associated with known genetic markers. As our strains have auxotrophic markers that allow us to distinguish different backgrounds, testing which phenotype they express and, from that, know whether the recombinant spores inherited their genotypes from one of the parental strains or whether they possess a mix of both. Namely, our strains are characterized by their ability, or inability, to grow on media lacking arginine, lysine and/or histidine. We can produce selective media by not adding one of these aminoacids to PMG plates and by verifying which of these media the samples derived from tetrad dissection can grow on, find out whether their phenotype is similar to that of one of the parental strains or a mix of both.

From this data we were able to calculate each cross' recombination rate by dividing the number of spores with a mixed genotype by the total number of spores.

Using an Analysis of Variance Model (3-Way ANOVA), we also estimated the impact each marker has on the recombinant spore's fitness, for all 4 crosses.



# 3. Results

---

## 3.1 Assessment of the number of cells picked during mutation accumulation

In order to investigate whether the genotype and karyotype affect the spontaneous mutation rate in fission yeast, we performed a mutation accumulation experiment (MA). In an MA, natural selection is reduced to a minimum, such that mutations accumulate close to the rate at which they are generated. To do so in microorganisms, this typically involves picking up one colony, re-streaking it in such a way that a new colony can be isolated after growth (Kibota and Lynch, 1996). This is called a bottleneck, whereby the population is reduced from several billion to a few cells, ideally only one. To make sure no more than one clone was being streaked, we estimated the number of cells carried over in each bottleneck. To do so, we mixed cells carrying three different fluorescent proteins, performed a bottleneck in the same manner as in the MA and checked how many colonies had mixed fluorescence (see Material and Methods, section 2.3).

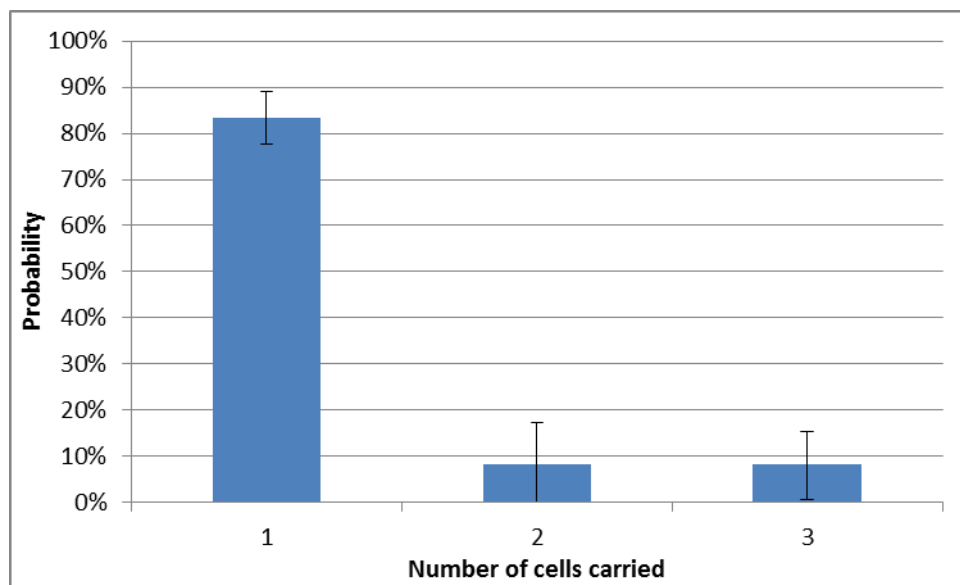


**Figure 3.1: Probability of isolating one, two or three cells per bottleneck. The error bars represent standard deviation from the mean. The data represents the pooled results of three experiments, each analyzing 96 streaks**

From the frequency of colonies with 1, 2 and 3 fluorescent proteins, we estimated the probability of isolating 1, 2 or 3 cells. On average, at each bottleneck we isolate a single cell 83% of the time ( $\pm 5\%$ ). This means 17% of the colonies originate from two or more cells. While this suggests that there can be some level of natural selection during the MA, that selection is still small, as the effective population

size is still close to unity. Even if two cells are dragged together during the streaking, it is very possible they were sister-cells, carrying similar, if not identical, genotypes. Furthermore, the chance of carrying more than one cell twice in a row for any given line is of less than 3%; the chance of doing so thrice in a row is about 0.5%. It is unlikely that a cell line will be subjected to multiple passages with this increase in selective pressure without complete isolation occurring in-between them.

We also tested whether the position of the colony in the petri dish affected the number of cells per bottleneck. We streak 12 lines on each YES agar plate, along a grid. The grid squares near the edge are smaller in size relative to the remaining areas. This smaller space could potentially lead to smaller streaks and, consequently, worse cell separation and fewer chances of obtaining colonies grown from isolated cells. Although the number of mixed colonies was indeed slightly higher in the corners than other regions (12 mixed colonies in corners, compared to 9 in all other fields), a  $\chi^2$  test indicated that the difference is non-significant (p-value > 0.1 ).

### **3.2 Mutation accumulation and competitions**

We performed the MA experiment for 12 different strains, each in 12 different replicate lines (144 evolution lines total). Of these 12 strains, 2 of them are direct descendants of the fission yeast type strain L972 where the only genetic engineering done to them was the introduction of a clonate resistance in the mating type locus (Avelar et al., 2013). One of them (SPP27) was a gift from the I. Tolic in Gottingen, Germany, while SPP26 was kept in the Portuguese Yeast Culture Collection under the number PYCC4197. These 2 strains have the same karyotype (A. T. Avelar, personal communication). However, whole genome sequencing done in our lab showed 16 genomic differences (not shown). From here on, these will be called the “Wild Type-like strains”. The other 10 strains represent pairs of strains where one of them has a chromosome rearrangement (1 inversion and 4 translocations) and the other is its wild type control. The controls have the same karyotype as the wild type and contain the loxP cassettes in the same locations as the rearranged strains. The construction of these strains and their karyotypes are described in Avelar 2013 and the materials and methods section. We use the same nomenclature for the rearrangements as in Avelar 2013.

We measured competitive fitness (see Materials and Methods, section 2.5) for all 12 strains at time 0 and for all 156 lines after 48 and after 144 bottlenecks (approximately 768 and 2304 generations respectively). The fitness values for all replicates of each strain and every line can be seen in Tables 6.2 through 6.14 in the Supplementary Material.

Figure 3.2 shows the fitness trajectory for the wild type strains SPP26 and SPP27. At time 0 they differ slightly in fitness with SPP27 being significantly less fit.

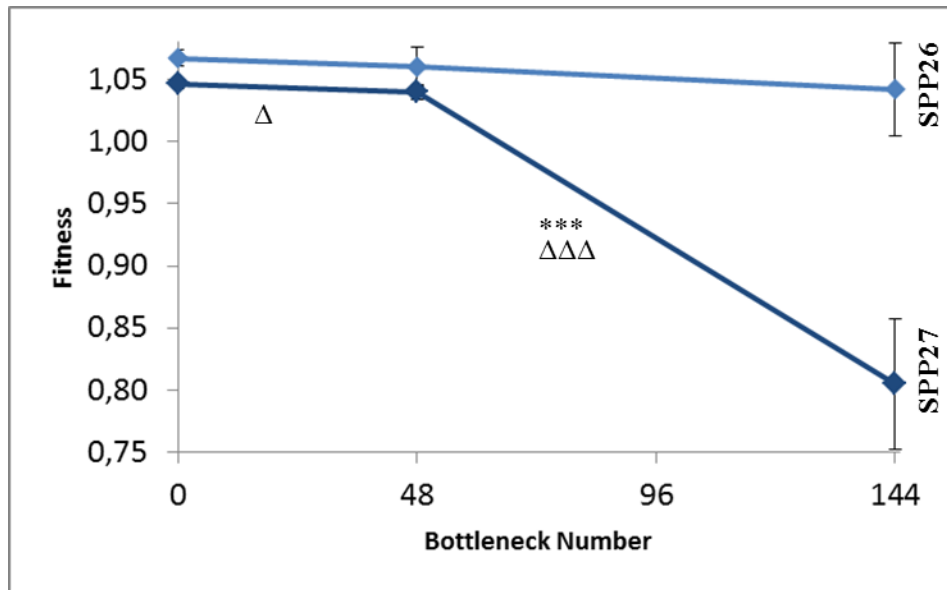


**Figure 3.2** Average fitness trajectories for strains SPP26 (in light blue) and SPP27 (in dark blue) across three different bottleneck numbers: B0, B48 and B144. For B0 the error bars represent experimental error from several measurements of the ancestral strain, while for B48 and B144 they represent the variance between all 12 cell lines per strain. \* shows a significant change in fitness distributions between both bottleneck numbers, while Δ does the same for fitness average. \*/Δ p-value < 0.05; \*\*/Δ Δ p-value < 0.01; \*\*\*/Δ Δ Δ p-value < 0.001. Bonferroni corrections were applied to all p-values.

Strain SPP26's fitness decreased from  $1.067 \pm 0.006$  (average  $\pm$  standard deviation) (normally distributed) at B0 to  $1.06 \pm 0.02$  (not normally distributed) at B48 and to  $1.04 \pm 0.04$  (not normally distributed) at B144. Strain SPP27's fitness decreased from  $1.046 \pm 0.004$  (normally distributed) at B0 to  $1.040 \pm 0.006$  (normally distributed) at B48 and to  $0.80 \pm 0.05$  (not normally distributed) at B144.

On average, SPP26 did not decrease in fitness, while SPP27 did, especially between bottlenecks 48 and 144.

Figure 3.3 shows the fitness trajectory for strains I2 and C2. At time 0 they differ slightly in fitness with C2 being significantly less fit.

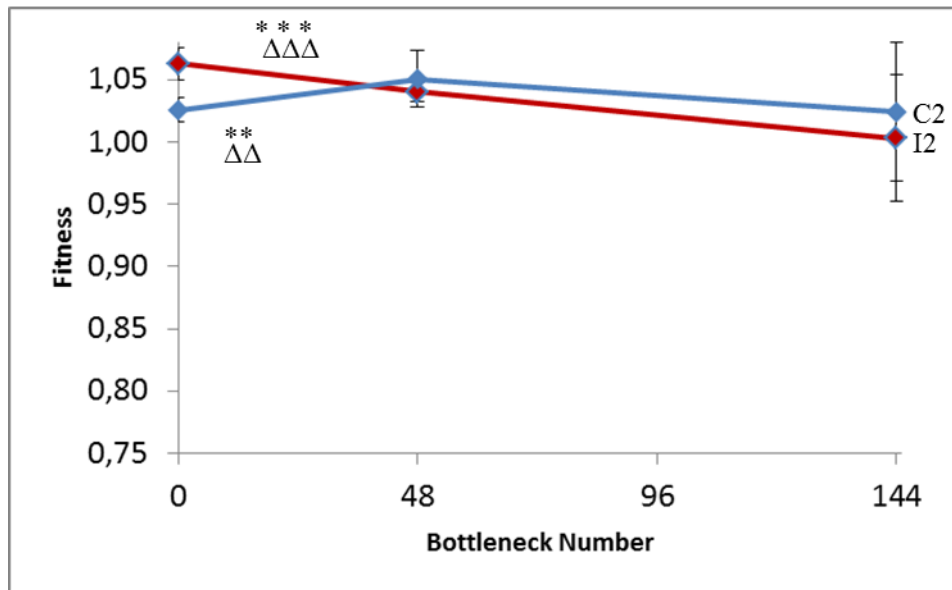


**Figure 3.3 Average fitness trajectories for strains C2 (blue) and I2 (red) across three different bottleneck numbers: B0, B48 and B144. For B0 the error bars represent experimental error from several measurements of the ancestral strain, while for B48 and B144 they represent the variance between all 12 cell lines per strain. \* shows a significant change in fitness distributions between both bottleneck numbers, while Δ does the same for fitness average. \*/Δ p-value < 0.05; \*\*/Δ Δ p-value < 0.01; \*\*\*/Δ Δ Δ p-value < 0.001. Bonferroni corrections were applied to all p-values.**

Next, we compared the fitness trajectories for Inversion 2 (I2 – see Introduction, section 1.3) and its control, C2. Strain I2’s fitness decreased from  $1.06 \pm 0.01$  (normally distributed) at B0 to  $1.040 \pm 0.007$  (normally distributed) at B48 and to  $1.00 \pm 0.05$  (not normally distributed) at B144.

Strain C2’s fitness increased from  $1.026 \pm 0.010$  (normally distributed) at B0 to  $1.05 \pm 0.02$  (not normally distributed) at B48 and decreased to  $1.02 \pm 0.06$  (not normally distributed) at B144.

I2B48 and C2B48 do not have significantly different averages nor distributions, and the same happens between I2B144 and C2B144. This indicates the two strains are converging.

We should note that C2 only has 11 lines past bottleneck 132. One of the lines went extinct (see Materials and Methods, section 2.2).

Figure 3.4 shows the fitness trajectory for strains T4 and C4. At time 0 they are significantly different in fitness, with T4 being less fit.

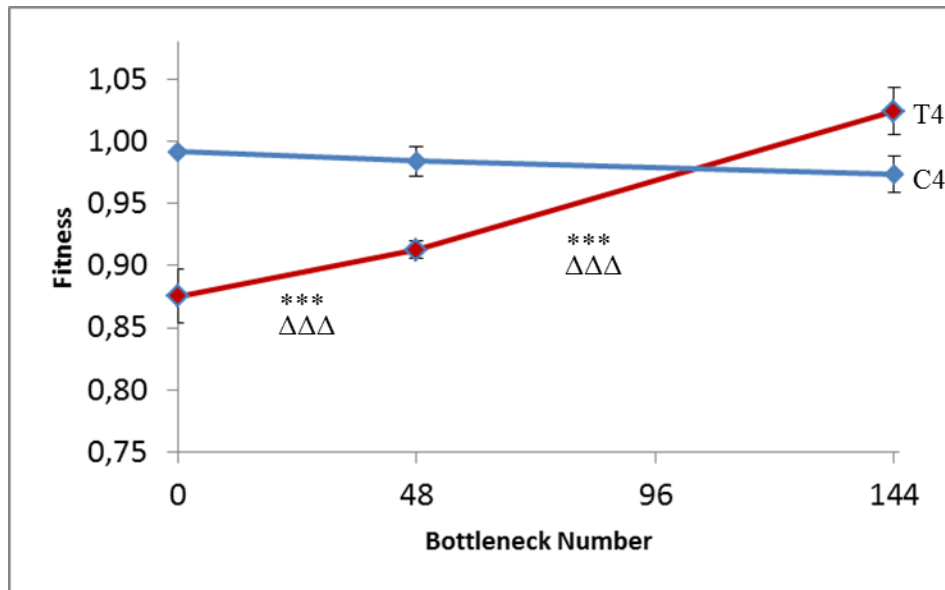


**Figure 3.4 Average fitness trajectories for strains C4 (blue) and T4 (red) across three different bottleneck numbers: B0, B48 and B144. For B0 the error bars represent experimental error from several measurements of the ancestral strain, while for B48 and B144 they represent the variance between all 12 cell lines per strain. \* shows a significant change in fitness distributions between both bottleneck numbers, while Δ does the same for fitness average. \*/Δ p-value < 0.05; \*\*/Δ Δ p-value < 0.01; \*\*\*/Δ Δ Δ p-value < 0.001. Bonferroni corrections were applied to all p-values.**

Strain T4’s fitness increased from  $0.88 \pm 0.02$  (normally distributed) at B0 to  $0.913 \pm 0.007$  (normally distributed) at B48 and to  $1.02 \pm 0.02$  (normally distributed) at B144. This result is unexpected and very surprising. Due to the absence of natural selection and the fact that most mutations are deleterious, we do not expect fitness to increase consistently in MA experiments.

Strain C4’s fitness decreased from  $0.992 \pm 0.003$  (normally distributed) at B0 to  $0.98 \pm 0.01$  (not normally distributed) at B48 and to  $0.97 \pm 0.01$  (normally distributed) at B144.

Figure 3.5 shows the fitness trajectory for strains T5, SPP20 and C5. At time 0 they are significantly different in fitness, with SPP20 being less fit than C5 and T5 being less fit than both.

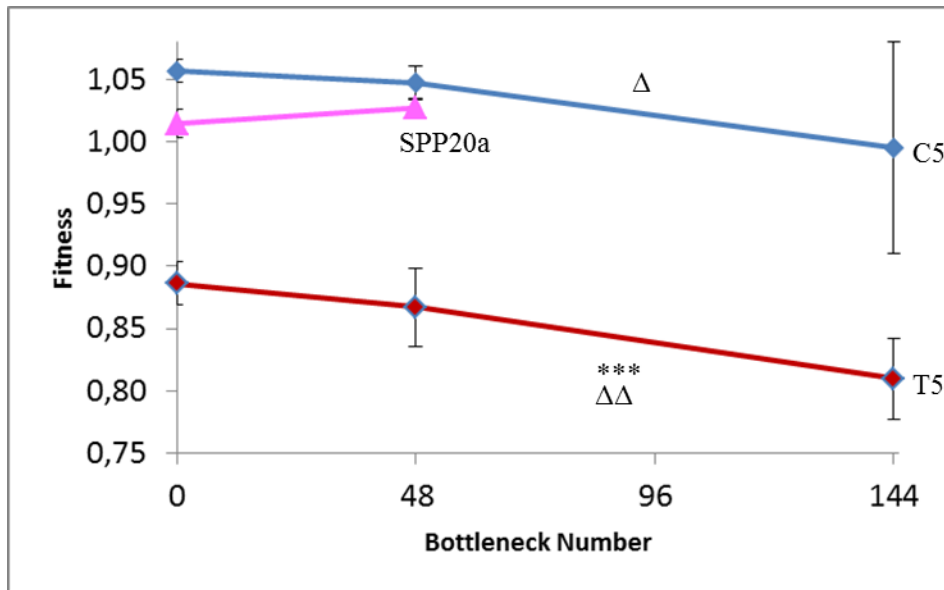


**Figure 3.5 Average fitness trajectories for strains C5 (blue), T5 (red) and SPP20 (pink) across three different bottleneck numbers: B0, B48 and B144 (not performed for SPP20 at this time). For B0 the error bars represent experimental error from several measurements of the ancestral strain, while for B48 and B144 they represent the variance between all 12 cell lines per strain. \* shows a significant change in fitness distributions between both bottleneck numbers, while Δ does the same for fitness average. \*/Δ p-value < 0.05; \*\*/Δ Δ p-value < 0.01; \*\*\*/Δ Δ Δ p-value < 0.001. Bonferroni corrections were applied to all p-values.**

In the case of translocation 5, its control C5 had a different mating type, namely h+, as stated before. In order to control for this, a new strain was created in the lab, referred to as SPP20 from here on out. SPP20 is identical to C5 with the exception of its mating type, which is h-. We also started to perform the MA propagation on this strain however, at the time of writing of this thesis, only 48 bottlenecks had elapsed.

Strain T5's fitness decreases from  $0.89 \pm 0.02$  (normally distributed) at B0 to  $0.87 \pm 0.03$  (not normally distributed) and to  $0.81 \pm 0.03$  (normally distributed) at B144.

Strain C5's fitness decreases from  $1.057 \pm 0.009$  (normally distributed) at B0 to  $1.05 \pm 0.01$  (normally distributed) at B48 and to  $1.00 \pm 0.09$  (not normally distributed) at B144.

Strain SPP20's fitness increases from  $1.02 \pm 0.01$  (not normally distributed) at B0 to  $1.027 \pm 0.007$  (normally distributed).

C5B48 and SPP20B48 do have significantly different distributions and medians (p-value < 0.01). However, we can see in the graph that they do seem to be converging. Unfortunately, due to its late start in the MA experiment, we cannot conclude whether its fitness trajectory will converge with C5's, whether it will keep increasing in fitness much like T4 or whether this increase is a temporary peak

before more deleterious mutations accumulate and its trajectory slopes downwards, as what happened with T8 in Figure 3.6.

Figure 3.6 shows the fitness trajectory for strains T8 and C8. At time 0 they are significantly different in fitness, with T8 being less fit.

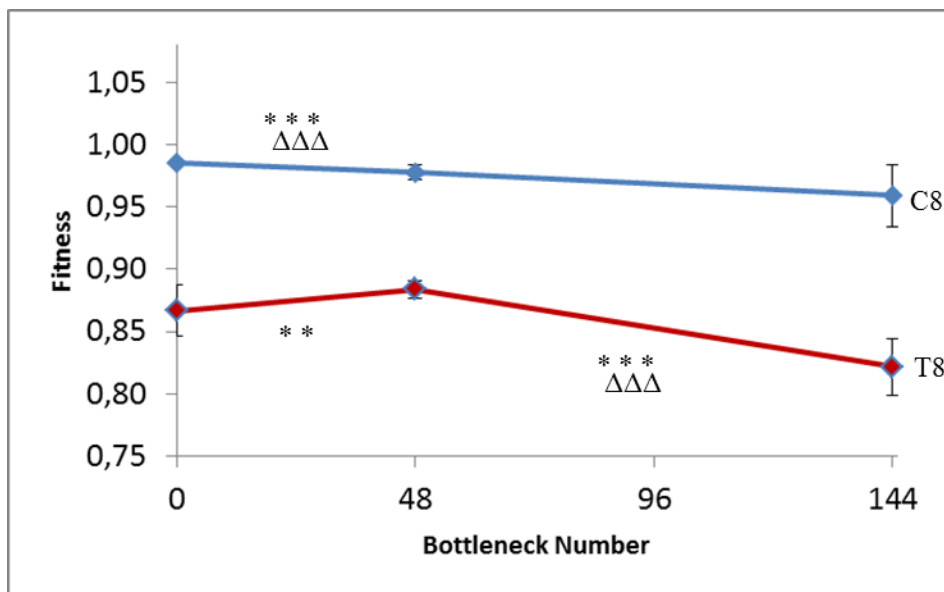


**Figure 3.6 Average fitness trajectories for strains C8 (blue) and T8 (red) across three different bottleneck numbers: B0, B48 and B144. For B0 the error bars represent experimental error from several measurements of the ancestral strain, while for B48 and B144 they represent the variance between all 12 cell lines per strain. \* shows a significant change in fitness distributions between both bottleneck numbers, while Δ does the same for fitness average. \*/Δ p-value < 0.05; \*\*/Δ Δ p-value < 0.01; \*\*\*/Δ Δ Δ p-value < 0.001. Bonferroni corrections were applied to all p-values.**

Strain T8's fitness increases from  $0.87 \pm 0.02$  (not normally distributed) at B0 to  $0.884 \pm 0.007$  (normally distributed) at B48 and decreases to  $0.82 \pm 0.02$  (normally distributed) at B144.

Strain C8's fitness decreases from  $0.986 \pm 0.003$  (normally distributed) at B0 to  $0.978 \pm 0.006$  (normally distributed) at B48 and to  $0.96 \pm 0.03$  (not normally distributed) at B144.

Like what happened with line C2.12, two lines of strain C8 went extinct before reaching B144. Line C8.7 went extinct on B132 and line C8.8 went extinct on B129.

Figure 3.7 shows the fitness trajectory for strains T10 and C10. At time 0 they differ slightly in fitness with C10 being significantly less fit.

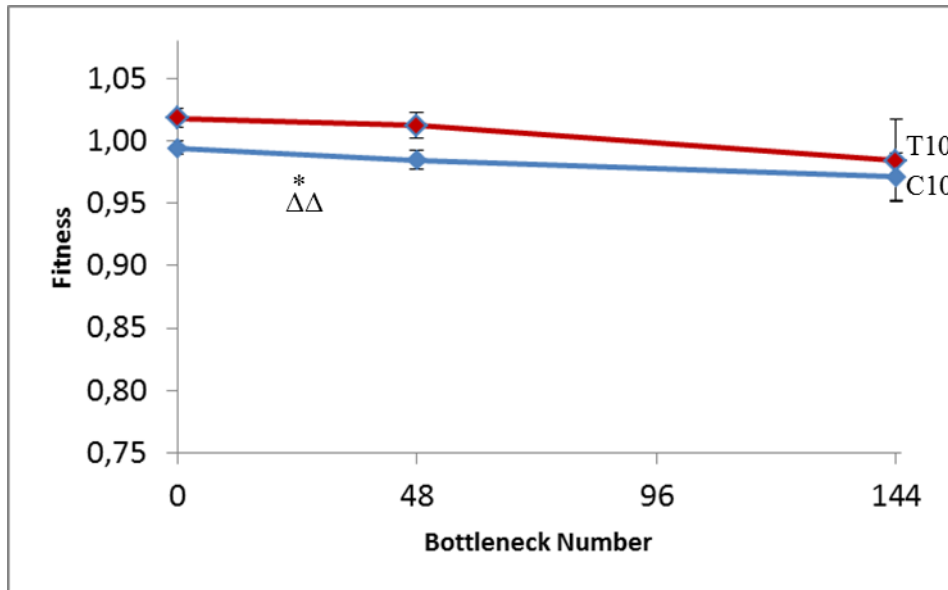


**Figure 3.7 Average fitness trajectories for strains C10 (blue) and T10 (red) across three different bottleneck numbers: B0, B48 and B144. For B0 the error bars represent experimental error from several measurements of the ancestral strain, while for B48 and B144 they represent the variance between all 12 cell lines per strain. \* shows a significant change in fitness distributions between both bottleneck numbers, while  $\Delta\Delta$  does the same for fitness average. \*/ $\Delta$  p-value < 0.05; \*\*/ $\Delta\Delta$  p-value < 0.01; \*\*\*/ $\Delta\Delta\Delta$  p-value < 0.001. Bonferroni corrections were applied to all p-values.**

Strain T10's fitness decreases from  $1.018 \pm 0.008$  (normally distributed) at B0 to  $1.01 \pm 0.01$  (not normally distributed) at B48 and to  $0.98 \pm 0.03$  (normally distributed) at B144.

Strain C10's fitness decreases from  $0.994 \pm 0.005$  (normally distributed) at B0 to  $0.985 \pm 0.007$  (normally distributed) at B48 and to  $0.97 \pm 0.02$  (not normally distributed) at B144.



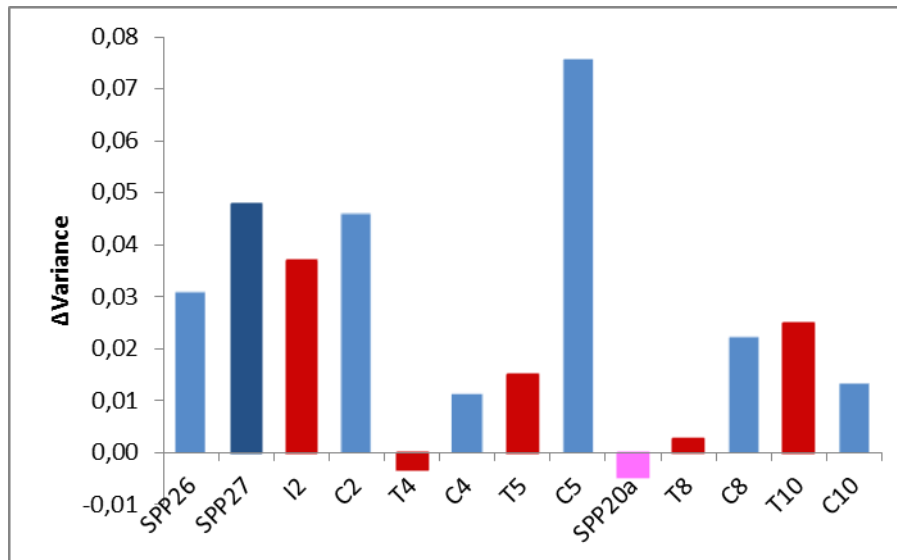


**Figure 3.8** Change in variance from B0 to B144 for each individual strain, with the exception of SPP20, which shows the difference in variance between B0 and B48.

With the accumulation of random mutations, the variance in fitness levels between each strain’s 12 lines tends to increase with the number of bottlenecks they experienced (Mukai, Chigusa, & Yoshikawa, 1964). Figure 3.8 shows the change in variance from bottleneck 0 (experimental error) to the end of the experiment at bottleneck 144. In general, the variance increased as expected, with notable exceptions.

Strains I2, T4 and T8 had a slightly lower variance at B48 than at B0, before it increased again at B144; of the three, only T4 didn’t have a higher variance at B144 than at B0.

Strain SPP20’s variance decreased slightly from B0 to B48. However, it is possible this is just a consequence of its measures being associated with a different experimental error.

**Table 3.1** Results from fitting the Analysis of Variance Model (ANOVA) comparing  $\Delta W$  (fitness at B144 subtracted from fitness at B0) all lines from different genomic backgrounds. Red indicates  $p\text{-value} < 0.05$ , yellow indicates  $0.01 > p\text{-value} > 0.001$  and green indicates  $0.001 > p\text{-value}$ . Bonferroni corrections were applied to all  $p\text{-values}$ .

	SPP26	SPP27	I2	C2	T4	C4	T5	C5	T8	C8	T10	C10
SPP26												
SPP27	9,8977E-09											
I2	5,36628972	2,1E-06										
C2	32,176518	6,227178	50,15595									
T4	1,5832E-10	3,29E-15	6,99E-10	0,847641								
C4	37,8229896	9,15E-10	1,297978	30,13474	1,89E-14							
T5	0,15037645	6,15E-07	24,05454	59,73462	8,47E-14	0,00212						
C5	13,4667456	0,000323	62,64657	51,60644	3,47E-06	8,015205	39,11081					
T8	9,3140652	6,9E-09	26,31535	42,04811	1,53E-14	0,273657	1,073373	35,86171				
C8	62,1447156	2,23E-08	5,511067	35,1945	5,8E-12	25,44505	0,069723	15,66261	6,039258			
T10	36,8132622	9,9E-09	11,22059	36,34719	6,96E-12	10,89927	0,370212	21,34037	23,6161	37,01266		
C10	57,6936096	5,1E-10	2,290222	31,08003	1,84E-14	32,49946	0,006733	10,21945	1,431345	49,90801	22,89706	

We compared the overall changes in fitness ( $\Delta W$ ) across all strains using an ANOVA (Table 3.1). Strain T4, as expected from its increase in fitness throughout MA, is significantly different from all other strains (p-value < 0.001), with the exception of C2 (p-value > 0.05), which had also demonstrated an overall increase in fitness level.

Strain SPP27 also behaves significantly differently from all other strains (p-value < 0.001) except for C2 (p-value > 0.05). The other Wild Type-like strain, SPP26, seems to behave significantly differently from strains SPP27 and T4.

With the exception of strains T4 and C4, none of the chromosomal alterations presented significantly different results from its respective control.

### 3.3 Mutation parameter estimation

Mutation accumulation experiments have been traditionally used to estimate the deleterious mutation rate and effects (Mukai, 1964; Kibota & Lynch, 1996; de Visser et al., 2011; Trindade et al., 2010). The method we used here is described in Gordo & Dionisio, 2005, and in the methods section. Briefly, the average decrease in fitness over time is proportional to the deleterious mutation rate ( $U_d$ ) and the mean effect of deleterious mutations ( $s_d$ ). The change in variance over time is also proportional to  $U_d$ , and to the square of  $s_d$ . From the change in fitness and its variance we can therefore estimate the average  $U_d$  and  $s_d$ . Since not all deleterious mutations have the same effect ( $s_d$  is not a constant), the estimate is an overestimate of  $s_d$  and an underestimate of  $U_d$  (Mukai, 1964; Gordo & Dionisio, 2005). In addition, the presence of beneficial mutations also leads to further underestimate of  $U_d$  and overestimate of  $s_d$  (Trindade et al., 2010). Given these limitations, this method gives us the upper bound for  $s_d$  and the lower bound for  $U_d$ . If we assume the variance in  $s_d$  and the rate of beneficial mutations is the same across backgrounds, we can use this method to directly compare  $U_d$  and  $s_d$  across strains, even if the confidence intervals for each parameter are large.

The parameters estimated for the strains used in this study can be seen in Table 3.2.

**Table 3.2 Fitness decline per mutation, arising mutations per generation, associated errors and mean mutation per generation of each strain.**

	$s_d$	$\delta s_d$	$U_d$	$\delta U_d$	$\lambda(G)$
SPP26	-0.05	0.01	7.8E-57	3.7E-54	0.003
SPP27	-0.016	0.008	2.80E-19	3.04E-16	0.127
I2	-0.04	0.02	6.64E-48	6.02E-45	0.009
C2	Not Applicable				
T4	Not Applicable				
C4	-0.011	0.004	1.14E-15	1.06E-12	0.011
T5	-0.012	0.007	1.002E-15	1.337E-12	0.054
C5	-0.12	0.05	3.07E-119	2.77E-116	0.004
T8	-0.01	0.01	8.59E-10	3.78E-06	0.075
C8	-0.026	0.008	1.74E-30	1.23E-27	0.007
T10	-0.03	0.01	3.7E-35	3E-32	0.008
C10	-0.016	0.005	3.13E-20	2.09E-17	0.010

Recent published data suggests that fitness, rather than genotype itself may affect the rate of accumulation of new mutations (Perfeito *et al.*, 2014; Kryazhimskiy *et al.*, 2014). So we investigated whether there was a relationship between initial fitness and the deleterious parameters estimate above. The correlations between initial fitness level and  $s_d$  and between initial fitness level and  $U_d$  are weak ( $R^2=0.10$  and  $R^2=0.23$ , respectively). Likewise, no correlation is detected between initial fitness and the change in fitness ( $\Delta W$ ) each strain experiences ( $R^2=0.17$ ).

There is a correlation between initial and final fitness. It is very weak due to the unexpected fitness changes of two of the strains (Figure 3.9).

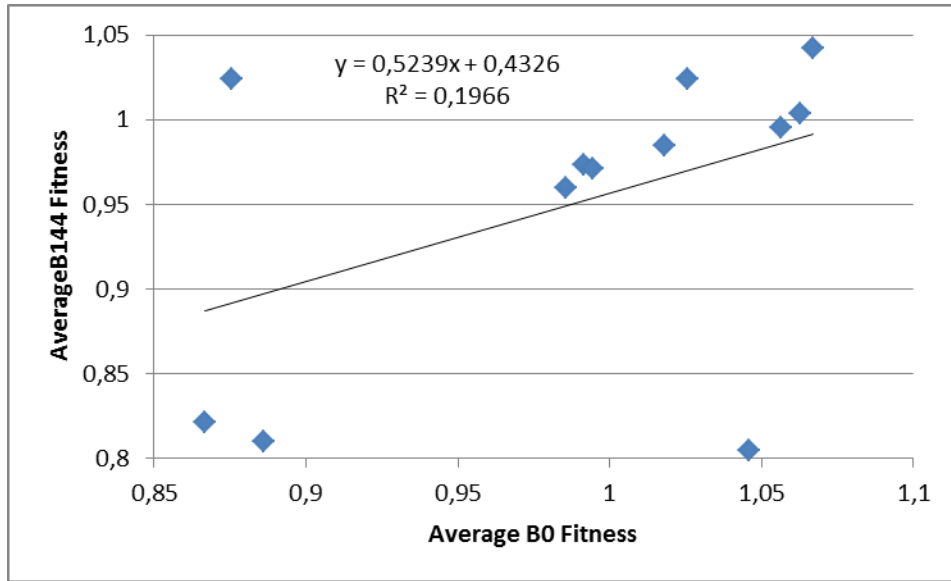


**Figure 3.9 Relationship between initial fitness (B0) and average fitness at B144.**

If we remove SPP27, which suffered from an inordinately steep decline in fitness throughout the experiment, and T4, which showed an unexpected increase in fitness, initial fitness values have a strong correlation with those of B144, as seen on Figure 3.10

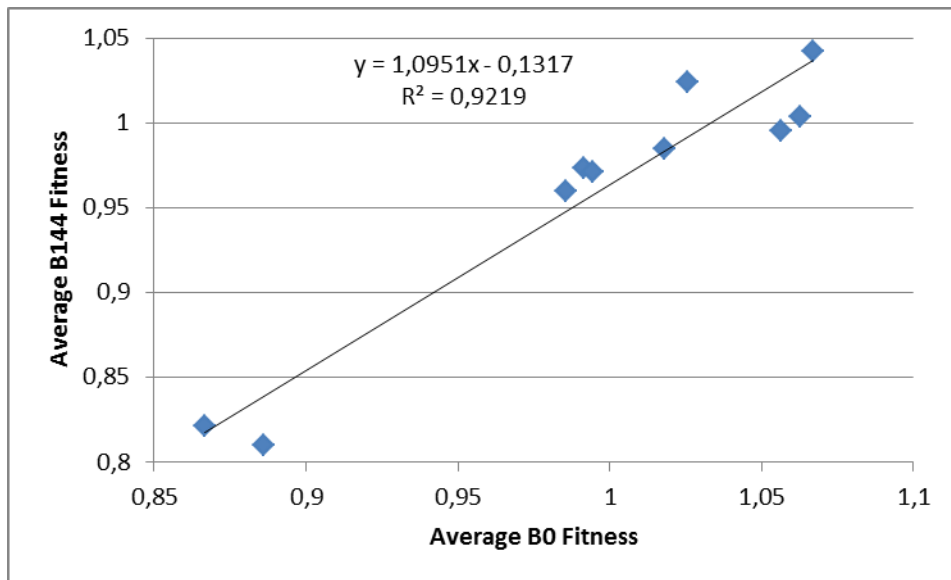


**Figure 3.10 Relationship between initial fitness (B0) and average fitness at B144 for strains SPP26, I2, C2, C4, T5, C5, T8, C8, T10 and C10.**

Similar correlations are observed even if we limit the data to the fitness values from B0 to B48 or from B48 to B144. In fact, if one tries to correlate solely B0's and B48's average fitness values, one obtains an  $R^2$  value higher than 0.9 even without excluding strains SPP27 and T4, as they only present this unexpected behavior after B48.

This shows that, despite change in fitness over the experiment, the less fit strains still remain, on average, less fit and the higher fit strains remain with a high fitness. This shows there has not been a strong convergence in fitness yet.

### **3.4 Test for genetic interactions between a rearrangement and accumulated mutations**

In order to test whether accumulated mutations interact to produce new effects (epistasis) or whether their effects are simply additive we must first separate them in an unmutated background. For the purpose, we chose ancestral strain C5 (C5B0), as it was the only strain in the experiment of the h+ mating type, capable of crossing with all others. To test for epistasis, we chose two lines from a translocation/control pair which showed the strongest differences by bottleneck 48: one line from T4B48, due to unexpected increases in fitness it suffered, and one line from its corresponding control, C4B48.

Additionally, we needed to distinguish the effects of the presence of mutation from the effects of crossing the two distinct genomic backgrounds themselves. We define as baselines the crosses between ancestral backgrounds, with no mutations in either: the cross between C5B0 and C4B0 and the cross between C5B0 and T4B0. After performing the four crosses, we isolated the resulting spores and competed them using the same protocol used to compete the MA lines, described previously.

Shapiro-Wilk test confirmed none of the four fitness frequency distributions are normally distributed, while Kolmogorov-Smirnov was used to compare them.

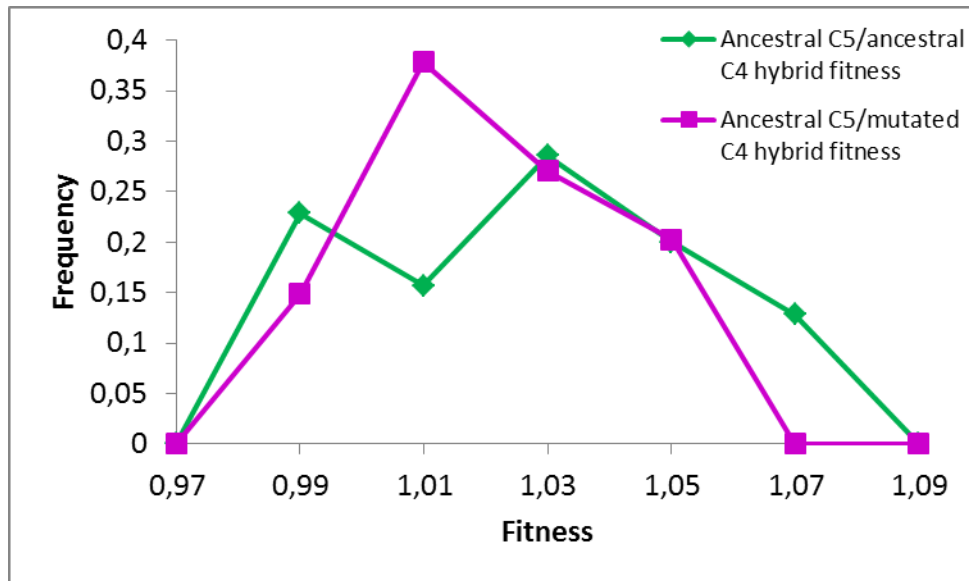


**Figure 3.11 Distribution of fitness frequencies of 2 sets of hybrids: those resulting from a cross between ancestral C5 and ancestral C4 strains (green line); and those resulting from the cross between ancestral C5 and a C4 line that underwent 48 bottlenecks (purple line).**

Figure 3.11 compares the distributions of fitness frequencies of C5a/C4a hybrids and C5/C4.3 hybrids. KS test indicates the two distributions are significantly different ( $0.01 < p\text{-value} < 0.005$ , Bonferroni corrected).

In the absence of epistasis, we expect the fitness of the spores to be the mean fitness of the parents. The mean fitness of C5B0 and C4B0 is  $1.02 \pm 0.03$  and the mean fitness of the spores is  $1.02 \pm 0.03$ . As the Wilcoxon test reports the two averages are not significantly different ( $p\text{-value} > 0.1$ ), we conclude there is not epistasis in this cross. The mean fitness of C5 and mutated C4 is  $0.99 \pm 0.03$ , while the mean fitness of the spores in this cross is  $1.01 \pm 0.01$ . The Wilcoxon test reports these two averages are significantly different ( $0.01 < p\text{-value} < 0.001$ ), so we conclude there is epistasis in this cross. Specifically, the mutations accumulated C4 seem to have a lower effect when separated, which is an indication of synergistic epistasis. We cannot compare the shape of the fitness distributions because we cannot know the expected distribution of spores under no epistasis. For that we would need to know how many mutations are different between the strains.

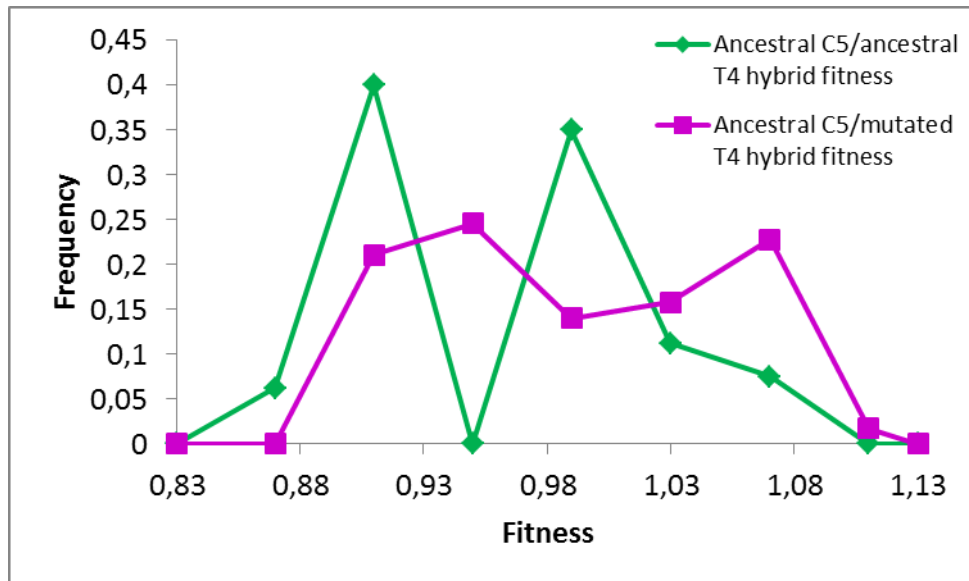


**Figure 3.12 Distribution of fitness frequencies of two sets of hybrids: those resulting from a cross between ancestral C5 and ancestral T4 strains (green line); and those resulting from the cross between ancestral C5 and a T4B48 strain (purple line).**

Figure 3.12 compares the distributions of fitness frequencies of C5a/T4a hybrids and C5/T4.11 hybrids. KS test indicates the two distributions are significantly different (p-value = 0.001, Bonferroni corrected).

The mean fitness of C5B0 and T4B0 is  $0.96 \pm 0.09$  and the mean fitness of the spores is  $0.94 \pm 0.06$ . As the Wilcoxon test reports the two averages are not significantly different (p-value > 0.1), we conclude there is not epistasis in this cross. The mean fitness of C5B0 and mutated T4 is  $0.93 \pm 0.06$ , while the mean fitness of the spores in this cross is  $0.97 \pm 0.06$ . The Wilcoxon test reports these two averages are not significantly different (p-value > 0.1), so we conclude there is no epistasis in this cross either.

Despite being both ancestral and evolved crosses being both bimodal, C5B0/T4.11 recombinant spores show a shift to the right, probably due to the accumulation of beneficial mutations in T4B48.

Individual fitness values for all replicates of every recombinant hybrid cross can be seen in Table 6.15, in the Supplementary Materials.

### 3.5 Comparisons between fitness and genotype

The presence of loxP sequences (See Introduction, section 1.3) is necessary to genetically engineer the controlled translocation and inversions (Avelar *et al.*, 2013). Such sequences were also inserted into the Control strains, silencing certain genes, such as those responsible for producing Histidine, Lysine and Arginine. These sequences are silencing these genes even on the control strains, onto which these

sequences were back-bred, only without incurring in the chromosomal rearrangement. Among the strains used to produce recombinant spores, C5 is deficient for the synthesis of histidine, while T4 and C4 cannot produce leucine or arginine. The leucine mutation is due to the mutation *leu1-32*, and not to a *loxP* site..

We genotyped the spores by checking their ability to grow in media without these aminoacids. From these data (seen in Table 6.1 in the Supplementary Material), we are able to calculate the recombination rate between genotypes with arginine, leucine and histidine auxotrophy. C5/C4.3 hybrids have a recombination rate of 0.757, while C5/T4.11 hybrids' own equals 0.526. When compared with free recombination, a rate of 0.5,  $\chi^2$  tests indicate the differences are not significant, with p-values between 0.9 and 0.5 and superior to 0.9, respectively. We conclude there is free recombination between these markers in our analysis.

We next wanted to know whether there was an association between the markers and fitness. This would indicate whether the deleterious mutations are associated with the breakpoints or not. We fitted an Analysis of Variance Model (3-way ANOVA), with fitness as the dependent variable:

**Table 3.3 Results of the fit of a 3-Way ANOVA correlating the presence of each auxotrophic marker in C5/C4.3 hybrid samples with those samples' fitness level as the dependent variable.**

\* p-value < 0.05; \*\* p-value < 0.01; \*\*\* p-value < 0.001

	P-value	
Arg	3.61e-15	***
Leu	0.000271	***
His	0.315059	
Arg:Leu	0.800091	
Arg:His	0.737356	
Leu:His	0.802355	
Arg:Leu:His	0.021355	*



**Table 3.4 Results of the fit of a 3-Way ANOVA correlating the presence of each auxotrophic marker in C5/T4.11 hybrid samples with those samples' fitness level as the dependent variable.**  
**\* p-value < 0.05; \*\* p-value < 0.01; \*\*\* p-value < 0.001**

	P-value	
Arg	0.000649	***
Leu	0.037133	*
His	0.238184	
Arg:Leu	0.973261	
Arg:His	0.378506	
Leu:His	0.793502	
Arg:Leu:His	0.004472	**

Genotypes containing the arginine marker have a highly significant effect on fitness level (see Tables 3.3 and 3.4). Arginine seems to be associated with higher fitness levels in both T4 and C4. This is likely an effect of the auxotrophy itself. The gene that allows cells to produce leucine also has a significant impact on fitness, more so for C5/C4.3 hybrid samples than for C5/T4.11 hybrid samples. Leucine is close to the mating type region and away from the breakpoints. The fact that it is associated with higher fitness may indicate fewer mutations accumulate in that area. The presence of all three genes at once is the only other of these genotypes that has a significant impact on fitness level.



# 4. Discussion

---

## 4.1 Mutation accumulation

This work gives us insight into the different effects of mutation accumulation in different chromosomal rearrangements of the same genome, and into the properties of those mutations in a species that offers untapped potential for this kind of studies. As is expected in experiments of this kind (Bateman, 1959; Mukai et al., 1964; Trindade et al., 2010), the fitness level of most lines decreased throughout the experiment and the variance between lines tended to increase (see Figures 3.2 through 3.8). However, we also observed an unexpected amount of beneficial mutations in some genotypes. One hypothesis to explain the abundance of beneficial mutations is that there is substantial natural selection operating during the MA. It could be, for example, that the population size at the bottleneck is high enough that rare mutants with beneficial mutations are able to survive it and outcompete the rest of the population. We measured the probability of carrying a single cell during the MA and shown it does not equal 100%. However, the chances of carrying more than one several times in a row are very low (see Figure 3.1). MA experiments have repeatedly shown their value when it comes to studying the mechanisms governing mutation and evolution (Bateman, 1959; Mukai et al., 1964; Trindade et al., 2010; Zeyl & DeVisser, 2001). But, it could be argued that when applied to unicellular organisms this method allows competition among the descendants of the original carried cell for the duration of the incubation. That is a problem with no easy solution. One hypothesis would be to perform the experiment in a microfluidic device whereby colonies are not allowed to grow past 1 or 2 cells.

## 4.2 Fitness trajectories

Our work with this technique produced some surprising results. T8 presented increases in fitness by B48, before all of its lines started accumulating further deleterious mutations that put their fitness at B144 at a level lower than they had been at B0 (see Figure 3.6). This is similar to what was observed in mutator *E. coli* previously (Trindade et al., 2010). Strains C2 and T4 showed a similar behavior at first (seen in Figures 3.3 and 3.4). However, by B144 strain C2 showed mostly an increase in variance, with some lines increasing and others decreasing in fitness. Meanwhile, all strain T4 lines kept increasing in fitness level throughout the experiment. Such an increase in fitness during an MA experiment has only been registered (to our knowledge) by (Stevens & Sebert, 2011) who performed the experiment in *Streptococcus pneumoniae*. We conclude this must be an effect of its chromosomal rearrangement, as its respective control behaved as expected, slightly decreasing in mean fitness (from  $0.992 \pm 0.003$  at B0 to  $0.974 \pm 0.014$  at B144). As such, strain T4's translocation can be seen as having

given it an increased propensity towards accumulating beneficial mutations. If this is the case, then the risk of carrying two or more cells on each bottleneck might be a leading factor in this increase. If the beneficial mutation rate of T4 is very high, then even in the small population sizes of the bottlenecks the beneficial mutations might be outcompeting the deleterious mutations. This increase leads to the conclusion that, in some cases, chromosomal rearrangements offer a massive adaptive advantage in a given medium. A strain that, by chance, received such a rearrangement and survived would tend to accumulate far more beneficial mutations than those without said rearrangement.

Alternatively, its atypical behavior could be explained if it had accumulated mutations that are deleterious in solid media (where we perform MA experiments), but have beneficial effects in liquid media (where we perform competition assays). It could also be that this specific translocation has altered the expression of chaperones, proteins capable of increasing fitness, or at least buffer fitness decrease, in the presence of deleterious mutations (Rutherford, 2003; Rudan *et al.*, 2015). Further work is planned to research the unique properties demonstrated by this strain.

Strains I2 and C2 presented an interesting case as well (see Figure 3.3). These two strains started out with significantly different ancestral medians and distribution, like the remaining pairs. However, by B48 both their medians and distributions were not significantly different ( $p$ -value  $> 0.1$ , Bonferroni corrected). This behavior is consistent until B144. This indicates both strains' evolutionary trajectories have converged.

The strong correlation between initial and final fitness levels could indicate the possibility of predicting a strain's final fitness knowing just its initial one (Figure 3.10). However, strains such as SPP27 and T4 show us that extreme increases or decreases on average fitness level confound this prediction (Figure 3.9). We must study what happens at increased bottleneck numbers to find out whether these unpredictable strains are exceptions to the rule, or whether all strains eventually tend towards extreme fitness changes as they accumulate more and more mutations, confounding any possible prediction.

The Wild Type-like strains, SPP26 and SPP27, served as controls for entirely different backgrounds, not just chromosomal rearrangements. They start at apparently similar but significantly different fitness levels, both in terms of average and distribution (see Figure 3.2). However, they accumulate mutations with rather different parameters. Strain SPP26's  $s_d$  is roughly 3 times bigger than SPP27's. On the other hand, SPP27's  $U_d$  is several orders of magnitude bigger than SPP26's. Ergo, the amount of mutations they are accumulating is very different, and the effects of these mutations are much more so. The fitness trajectories of these Wild Type-like strains also diverge farther than those of any of our rearrangements and respective controls. This is not unexpected, as these two strains have been cultivated in different laboratories for decades. They must have accumulated different mutations throughout the decades as they adapted to different media, even prior to our own MA experiment. In

fact, whole genome sequencing done in our lab showed 16 genomic differences (not shown) (L. Perfeito, personal communication). These results show that prior mutational load can have a larger total effect on fitness trajectories than any of the chromosomal rearrangements we used. The divergence between these strains' fitness trajectories was larger than the ones observed between the chromosomal rearrangements and their respective controls, this fact does not mean chromosomal rearrangements have little effect on a strain's evolution. Since these strains have completely identical genetic material, merely rearranged differently, we are effectively isolating just the effects rearrangements have on their evolutionary trajectories.

Despite the shortcomings of the MA analysis mentioned above, we are able to show that chromosomal rearrangements can alter the speed of evolution as shown in table 3.1. The ANOVA shown there indicates that although most rearrangements do not provide significantly different *changes in fitness* ( $\Delta W$ ) compared to their respective controls (p-value > 0.05), some do. Namely strains T4 and C4 have significantly different  $\Delta W$  from each other (p-value < 0.001). In fact, T4 shows significantly different  $\Delta W$  from all strain except C2, many of whose lines presented increases in fitness as well. Strain C4 has a significantly different  $\Delta W$  from T4 and from T5 as well (0.01 > p-value > 0.001). T5's  $\Delta W$ , in turn, is significantly different from C4's and from C10's as well. This could be because both C4 and C10 had a relatively small  $\Delta W$  when compared to T5, as they mostly increased in variance.

As for the Wild-Type like strains, SPP26 and SPP27 show significantly different  $\Delta W$  from each other (p-value < 0.001) as well, which could be explained by their different backgrounds, confirming our conclusions stated above. However, while SPP26's  $\Delta W$  is significantly different from SPP27's and T4's, SPP27's  $\Delta W$  is significantly different from all other strains' except C2's (p-value > 0.05). This could indicate that SPP26's genetic content is more similar to the rearrangements and their controls than SPP27's.

### **4.3 Recombinant hybrids**

Even if the chromosomal rearrangement decreases the strain's fitness to the point it cannot compete against others in the same system, these beneficial mutations can also be transmitted to fitter genotypes through sexual reproduction. We quantified the effect of this transmission by producing recombinant spores between strains that accumulated mutations and one strain that did not. We have as an example the distributions of fitness frequencies of C5a/T4a hybrids and C5/T4.11 hybrids (as seen in Figures 3.11 and 3.12). The distribution for C5a/T4a hybrids appears to be bimodal. The spores produced from these crosses tend to have low viability, as many spores die or, alternatively, tetrads are formed with less than 4 spores (see Table 6.1 in the Supplementary Materials). The alterations to tetrad formation are such that some tetrads from these crosses were formed with 5

spores, a phenomenon that has never been recorded (to our knowledge). The fifth spore, however, did not survive, as it probably contained no genetic material. These deficiencies in tetrad formation confirm the meiotic load associated with translocations (Avelar 2013). In this case, cells must inherit either both chromosomes 2 and 3 from parental strain C5 or both from parental line T4. Inheriting one from each of the strains could possibly lead to missing housekeeping genes, in which case the two distributions represented correspond to the two strains: one at lower fitness levels for T4 and one at higher ones for C5. The inheritance of beneficial mutations could occur through crossing-over occurring between homologous regions of chromosomes 2 and 3. These would allow one strain to receive portions of genetic material from the other's chromosomes without losing its own set and, with them, essential genes. Alternatively, they could exchange mutations accumulated on chromosome 1, as it is freely interchangeable between both strains.

The effect of beneficial mutations can be seen when that distribution is compared to that of C5/T4.11 hybrids. Both distributions of fitness frequencies present similar bimodal distributions, but that derived from mutated T4.11 parentals is shifted to the right. This means that, on average, the C5/T4.11 hybrids will be fitter than C5a/T4a hybrids. Once again, this shows how a chromosomal rearrangement can provide an adaptive advantage, not just for the cells that carry it but also for other strains in the same environment, as the beneficial mutations accumulated by such a rearrangement can then increase the fitness of strains with other karyotypes.

While the mutations accumulated by T4.11 do not seem to have epistatic effects, being merely additive, those accumulated by C4.3 do. C5a/C4a hybrids' distribution is also slightly bimodal, as they also present the tetrad formation deficiencies, though not in the same scale as C5a/T4a hybrids'. However, C5/C4.3 hybrids' present a more normalized distribution (although still not normal, tested with Shapiro-Wilk,  $0.01 > p\text{-value} > 0.005$ ). This could indicate that these mutations are not as deleterious when separated compared to when they're together in the same genome. This could create an effect where the increased number of lower fitness cells "covers" the gap in the bimodal distribution.

Using these recombinant spores we were also able to verify that fitness can be correlated with the presence of certain auxotrophic markers (see Tables 3.3 and 3.4). Strains capable of producing arginine, of producing leucine or of producing arginine and leucine and histidine tend to have higher fitness values than those that don't. This indicates that, even in rich media with all these aminoacids present, the ability to produce them still allows *S. pombe* cells to reproduce faster in their environment when compared with strains that can't. Mutations that affect these genes will thusly have a strong effect on the fitness level.

#### 4.4 Mutation parameters

Beneficial mutations have been shown to bias the estimates of mutation parameters, leading to an overestimate of the effect of deleterious mutations ( $s_d$ ) and an underestimate of the deleterious mutation rate ( $U_d$ ) (Keightley, 1998). In this study, however, some lines had an abundance of beneficial effects high enough to lead us to be unable to estimate these parameters in the first place. In the future, we will have to use models capable of estimating the effects of beneficial mutations, or of separating the effects of deleterious and beneficial mutations.

Strain SPP26 and SPP27's  $U_d$  and  $s_d$  values are not the only ones that are very small (see Table 3.2). In general, our estimated  $U_d$  is far lower than what had previously been estimated in *Saccharomyces cerevisiae*, and those values had been assumed to be underestimates. Meanwhile our estimated  $s_d$  was similarly several times smaller than those studies' published values, although those values might have been overestimated (Wloch *et al.*, 2001). As this experiment had never been performed using *S. pombe* strains, it might be possible that *S. pombe* has a lower predisposition towards deleterious mutations. Despite both being species of yeast, *Saccharomyces cerevisiae* and *S. pombe* have several genomic differences that might account for this discrepancy (see Introduction, section 1.2). We could also simply be using the wrong predictive model for these strains. Specifically, we should use one that incorporates beneficial as well as deleterious mutations. It has been suggested that comparisons of DNA sequences might be a better tool for experimental investigation of spontaneous mutations, as it is a method that is capable of uncovering even the smallest of mutations (Wloch *et al.*, 2001) that might not have individually visible effects on fitness. However, whole genome sequence will tell us nothing about evolutionary outcome of mutations without direct fitness measurements as we do here.

#### 4.5 Future Work

Due to the ambitious scope of our work, we could not perform all the test and experiments we desired within the timeframe of this Thesis. We have many ways in which we are planning to deepen our research in the future.

It might be useful to repeat some competition assays, as there were competition replicates where only 3 timepoints were used for the linear regression (as they hit frequencies of 99% or 1% before the fourth timepoint). This happened with particular frequency for the recombinant hybrid samples.

We will keep following the evolutionary trajectory of each line as they keep accumulating mutations, by measuring their fitness levels at bottleneck levels past B144.

The estimated number of generations per bottleneck was calculated only for B0 samples. It is necessary that we verify whether the number of generations experienced by each colony in 48 hours is constant throughout mutation accumulation.

To better understand our results, we could sequence mutated lines, so as to understand what mutations occurred and how they are affecting fitness. Of particular interest is the sequencing of T4 cell lines, for their unusual number of beneficial mutations and other unexpected behaviors. The same could be done for recombinant hybrids, which would help us to associate each mutation with a particular effect on fitness. Sequencing might also help us explain how and why crosses with T4 strains (both C5a/T4a hybrids and C5/T4.11 hybrids) produced tetrads with 5 spores.

And due to this unexpected behavior on the part of T4 lines, we plan to perform competitions for T4 cell lines in solid medium instead of liquid medium. Devising such an experiment would allow us to verify whether the mutations they accumulated are beneficial in both types of media. It could be that it did accumulate deleterious mutations on YES agar and that those mutations, for some reason, confer an adaptive advantage when growing in liquid media. As we perform our competition assays exclusively in liquid media, we would only observe the beneficial effects of these mutations. If the fitness levels of strain T4's lines are demonstrated lower when competed in a solid medium, it might indicate we are looking at a case of 100% antagonistic pleiotropy.

We would like to also test the presence of auxotrophic markers for the ancestral crosses, C5a/T4a hybrids and C5a/C4a hybrids. Likewise, it might be informative to also perform this test for mutated C4.3 and T4.11, as we took our conclusions under the assumption that these lines keep the same auxotrophic markers as their ancestral strains.



# 5. Bibliography

---

## 5.1 Journal references

- Avelar, A. T. (2012). *Chromosomal structure : a selectable trait for evolution*.
- Avelar, A. T., Perfeito, L., Gordo, I., & Ferreira, M. G. (2013). Genome architecture is a selectable trait that can be maintained by antagonistic pleiotropy. *Nature Communications*, 4(October 2015). <http://doi.org/10.1038/ncomms3235>
- Barton, N. H. (2010). Mutation and the evolution of recombination. *Philosophical Transactions of the Royal Society B: Biological Sciences*, 365(1544), 1281–1294. <http://doi.org/10.1098/rstb.2009.0320>
- Bateman, A. J. (1959). The Viability of Near-normal Irradiated Chromosomes. *International Journal of Radiation Biology and Related Studies in Physics, Chemistry and Medicine*, 1(2), 170–180. <http://doi.org/10.1080/09553005914550241>
- Bateson, B. (2009). An Address on Mendelian Heredity and its application to Man. Delivered before the Neurological Society, London, I. ii. 1906. In *William Bateson, Naturalist* (pp. 181–200). Cambridge University Press. Retrieved from <http://dx.doi.org/10.1017/CBO9780511693946.004>
- Brown, W. R. a., Liti, G., Rosa, C., James, S., Roberts, I., Robert, V., ... Fay, J. C. (2011). A Geographically Diverse Collection of *Schizosaccharomyces pombe* Isolates Shows Limited Phenotypic Variation but Extensive Karyotypic Diversity. *G3 & #58; Genes/Genomes/Genetics*, 1(7), 615–626. <http://doi.org/10.1534/g3.111.001123>
- Carter, Z. and Delneri, D. (2010), New generation of loxP-mutated deletion cassettes for the genetic manipulation of yeast natural isolates. *Yeast*, 27: 765–775. doi: 10.1002/yea.1774
- Chevin, L.-M. (2011). On measuring selection in experimental evolution. *Biology Letters*, 7(2), 210–213. <http://doi.org/10.1098/rsbl.2010.0580>
- Colato, a, & Fontanari, J. F. (2001). Soluble model for the accumulation of mutations in asexual populations. *Physical Review Letters*, 87(23), 238102. <http://doi.org/10.1103/PhysRevLett.87.238102>
- De Visser, J. a. G. M., Cooper, T. F., & Elena, S. F. (2011). The causes of epistasis. *Proceedings of the Royal Society B: Biological Sciences*. <http://doi.org/10.1098/rspb.2011.1537>
- Darwin, C. (1859). *On the Origin of Species by Means of Natural Selection, or the Preservation of Favoured Races in the Struggle for Life*. John Murray, Albemarle Street, London
- Dunwell, J. M. (2007). 100 Years on: a Century of Genetics. *Nature Reviews. Genetics*, 8(March), 231–235. <http://doi.org/10.1038/nrg2064>
- Farlow, A., Long, H., Arnoux, S., Sung, W., Doak, T. G., Nordborg, M., & Lynch, M. (2015). The spontaneous mutation rate in the fission yeast *Schizosaccharomyces pombe*. *Genetics: Early Online*, 14.

- Forsburg, S. L., & Rhind, N. (2006). Basic methods for fission yeast. *Yeast*, 23(3), 173–183. <http://doi.org/10.1002/yea.1347>
- Gordo, I., & Dionisio, F. (2005). Nonequilibrium model for estimating parameters of deleterious mutations. *Physical Review E*, 71(3), 031907. <http://doi.org/10.1103/PhysRevE.71.031907>
- Keightley, P. D. (1998). Inference of genome-wide mutation rates and distributions of mutation effects for fitness traits: A simulation study. *Genetics*, 150(3), 1283–1293.
- Kibota, T. T., & Lynch, M. (1996). Estimate of the genomic mutation rate deleterious to overall fitness in *E. coli*. *Nature*. <http://doi.org/10.1038/381694a0>
- Kryazhimskiy, S., Rice, D. P., Jerison, E. R., & Desai, M. M. (2014). Global epistasis makes adaptation predictable despite sequence-level stochasticity. *Science*, 344(6191), 1519–22. <http://doi.org/10.1126/science.1250939>
- Morran, L. T., Parmenter, M. D., & Phillips, P. C. (2009). Mutation load and rapid adaptation favour outcrossing over self-fertilization. *Nature*, 462(7271), 350–352. <http://doi.org/10.1038/nature08496>
- Mukai, T., Chigusa, S., & Yoshikawa, I. (1964). the Genetic Structure of Natural Populations of *Drosophila Melanogaster*. I. Spontaneous Mutation Rate of Polygenes Controlling Viability. *Genetics*, 50(500), 1–19.
- Nurse, P. (2000). Fission Yeast Handbook: Welcome to the lab. Retrieved from [http://research.stowers.org/baumannlab/documents/Nurselab\\_fissionyeasthandbook.pdf](http://research.stowers.org/baumannlab/documents/Nurselab_fissionyeasthandbook.pdf)
- Perfeito, L., Sousa, a., Bataillon, T., & Gordo, I. (2014). Rates of Fitness Decline and Rebound Suggest Pervasive Epistasis. *Evolution*, 68(1), 150–162. <http://doi.org/10.1111/evo.12234>
- Rudan, M., Schneider, D., Warnecke, T., & Krisko, A. (2015). RNA chaperones buffer deleterious mutations in *E. coli*. *eLife*, 4, 1–16. <http://doi.org/10.7554/eLife.04745>
- Rutherford, S. L. (2003). Between genotype and phenotype: protein chaperones and evolvability. *Nature Reviews Genetics*, 4(4), 263–274. <http://doi.org/10.1038/nrg1041>
- Stevens, K. E., & Sebert, M. E. (2011). Frequent Beneficial Mutations during Single-Colony Serial Transfer of *Streptococcus pneumoniae*. *PLoS Genetics*, 7(8), e1002232. <http://doi.org/10.1371/journal.pgen.1002232>
- Trindade, S., Perfeito, L., & Gordo, I. (2010). Rate and effects of spontaneous mutations that affect fitness in mutator *Escherichia coli*. *Philosophical Transactions of the Royal Society of London. Series B, Biological Sciences*, 365(1544), 1177–1186. <http://doi.org/10.1098/rstb.2009.0287>
- Wloch, D. M., Szafraniec, K., Borts, R. H., & Korona, R. (2001). Direct Estimate of the Mutation Rate and the Distribution of Fitness Effects in the Yeast *Saccharomyces cerevisiae*. *Genetics*, 159(2), 441–452. Retrieved from <http://www.genetics.org/content/159/2/441.abstract>
- Yanagida, M. (2002). The model unicellular eukaryote, *Schizosaccharomyces pombe*. *Genome Biology*, 3(3), COMMENT2003. <http://doi.org/10.1186/gb-2002-3-3-comment2003>
- Zeyl, C., & DeVisser, J. a. (2001). Estimates of the rate and distribution of fitness effects of spontaneous mutation in *Saccharomyces cerevisiae*. *Genetics*, 157(1), 53–61.

## 5.2 Electronic references

Fonnesbeck, Christopher J. 2014. 12. Appendix: Markov Chain Monte Carlo. Version 06 October 2015.  
<http://pymcmc.readthedocs.org/en/latest/theory.html> in PyMC User's Guide,  
<http://pymcmc.readthedocs.org/en/latest/index.html#>.

Becton, Dickinson and Company. 2011. BD LSRFortessa brochure. Version 06 October 2015.  
<http://www.helsinki.fi/biosciences/corefacilities/flowcytometry/BD%20LSRFortessa%20brochure.pdf>  
in University of Helsinki <https://www.helsinki.fi/en>.



# 6. Supplementary Materials

**Table 6.1 C5+C4.3 and C5+T4.11 samples organized by tetrad the spore originated from and marked with parental or mixed phenotypes.**

C5+C4.3												
	1	2	3	4	5	6	7	8	9	10	11	12
A	1	3*	7	9	11	14	16	18	20	22		
B	1	4*	7	9	11	14	16	18	20	22		
C	2	5	7	9	11	14	16	18	20	22		
D	2	5	7	9	12	15	16	18	20	22		
E	3	5	8	10	12	15	17	19	21			
F	3	6	8	10	12	15	17	19	21			
G	4	6	8	10	13		17	19	21			
H	4	6	8	10	13		17	19	21			
											phenotypes:	C5
												C4/T4
												mixed

C5+T4.11												
	1	2	3	4	5	6	7	8	9	10	11	12
A	1	3	6	10	13	15	18	24				
B	1	3	6	10	13	15	19					
C	1	3	7	10	13	15	20					
D	1	3	7	11	13	15	21					
E	2	4	8	11	14	16	22					
F	2	4	8	12	14	16	22					
G	2	5	9	12	14	17	23					
H	2	5	9	12	14	17	23					

**Table 6.2 Individual fitness values for all replicates of strain SPP26 and corresponding lines, across bottlenecks 0, 48 and 144. Blank cells represent replicates that could not be measured or were used as controls.**

	B0			B48				B144	
SPP26	1,070553	1,067552	Line 1	1,019171	1,027684	1,014051	Line 1	1,000151	1,001112
	1,069317	1,076213		1,003434	1,034105	1,013769	Line 2	1,052357	1,076908
	1,067401	1,075013		0,965149	1,03528	1,017146	Line 3	1,029227	1,007281
	1,05919	1,083449		1,013152	1,041062	1,020648	Line 4	1,050205	1,061642
	1,069682	1,075433	Line 2	1,053264	1,076019	1,054668	Line 5	1,078836	1,048837
	1,067561	1,069876		1,050529	1,082458	1,065372	Line 6	1,075901	
	1,067244	1,064682		1,041838	1,064066	1,061515	Line 7	0,955882	0,958184
	1,066098	1,074327		1,053355	1,079214	1,059819	Line 8	1,089549	1,073497
	1,064075	1,065	Line 3	1,044524	1,093165	1,063576	Line 9	1,073165	1,070523
	1,071757	1,066125		1,052588	1,081591	1,06147	Line 10	1,054318	1,053931
	1,069873	1,068603		1,050943	1,089437	1,053073	Line 11	0,999184	0,999516
	1,073766	1,075903		1,052804	1,100531	1,060372	Line 12	1,072831	1,050856
	1,058194	1,059086	Line 4	1,052366	1,088604	1,067348			
	1,072451	1,071009		1,056544	1,106263	1,058896			
	1,061092	1,080654		1,052955	1,089927	1,06555			
	1,069924	1,07052		1,069649	1,111142	1,073814			
	1,067411	1,066398	Line 5	1,041377	1,063755	1,044699			
	1,067835	1,077938		1,042492	1,067353	1,058481			
	1,057667	1,070919		1,044271	1,103501	1,056136			
	1,056553	1,081567		1,056149	1,085984	1,062047			
		1,063506	Line 6		1,075789				
	1,056839	1,060651		1,056152	1,073936	1,057149			
	1,061512	1,074554		1,050347	1,085593	1,058184			
	1,057708	1,063452		1,064047	1,088958	1,065618			
		1,0612	Line 7	1,028432	1,023572	1,032103			
						1,041913			
	1,061727	1,074611		1,03786	1,05026	1,032079			
	1,063594	1,063788		1,049851	1,04563	1,044799			
	1,068159	1,060169	Line 8	1,047579	1,081652	1,061303			
	1,058141	1,072284		1,053421	1,073878	1,053649			
	1,067174	1,067688	Line 9	1,069811	1,082752	1,06235			
	1,067491	1,069181		1,051868	1,073013	1,053555			
	1,059287	1,072774		1,055988	1,072844	1,063358			
	1,057646	1,070629		1,057389	1,052347	1,062625			
	1,061545		Line 10	1,058014					
	1,058327	1,065555		1,05389	1,103931	1,060291			
	1,065831	1,059813		1,05037	1,07568	1,057787			
	1,063464	1,065648		1,044597	1,102983	1,058604			
1,069942	1,08104	Line 11	1,066184	1,085302	1,060329				
1,063073	1,063372		1,052638	1,082118	1,059148				
1,065464	1,06683		1,056632	1,09902	1,057673				
1,067	1,075063		1,052327	1,124493	1,058907				
1,063244	1,072316	Line 12	1,060963	1,077381	1,06843				
1,074748	1,058819		1,054319	1,101611	1,060791				
1,066432	1,071519		1,057608	1,087871	1,054212				
1,068542	1,070079		1,049844	1,102062	1,060601				
1,059087	1,069816		1,053387	1,090762	1,059757				

**Table 6.3 Individual fitness values for all replicates of strain SPP27 and corresponding lines, across bottlenecks 0, 48 and 144. Blank cells represent replicates that could not be measured or were used as controls.**

	B0			B48				B144	
SPP27	1,049262	1,058703	Line 1	1,045728	1,05655	1,049078	Line 1	0,820284	0,839589
	1,047641	1,052886		1,027885	1,057311	1,05167	Line 2	0,837191	0,814576
	1,04771	1,052757		1,033231	1,049428	1,04541	Line 3	0,839346	0,813945
	1,03812	1,049258		1,037591	1,053485	1,044394	Line 4	0,758818	0,762619
		1,049464	Line 2		1,057479		Line 5	0,754577	0,758159
	1,045123	1,045381		1,028932	1,065448	1,042256	Line 6	0,864756	0,789772
	1,041116	1,036486		1,015282	1,045941	1,045753	Line 7	0,794713	0,936897
	1,039163	1,051195		1,024148	1,061607	1,036233	Line 8	0,822885	0,844965
	1,044911	1,050827	Line 3	1,029692	1,042903	1,043628	Line 9	0,841086	0,793104
						1,034184	Line 10	0,593393	0,732253
	1,040256	1,047084		1,024589	1,038742	1,030514	Line 11	0,858588	0,823662
	1,04141	1,050285		1,024608	1,0312	1,040704	Line 12	0,790449	0,833002
	1,052029	1,050395	Line 4	1,026282	1,053219	1,035476			
	1,043236	1,038525		1,030133	1,052347	1,034679			
	1,040435	1,044873		1,029147	1,050321	1,032506			
	1,04901	1,058288	Line 5	1,028102	1,050177	1,052325			
	1,039766	1,055606		1,024544	1,046932	1,042647			
	1,042808	1,045548		1,032119	1,049417	1,042382			
	1,039923			1,038475					
	1,050035	1,046572	Line 6	1,01212	1,035461	1,036706			
	1,047384	1,040684		1,013824	1,035977	1,027236			
	1,04356	1,046438		1,020971	1,035145	1,021975			
	1,042062	1,049027		1,009359	1,039285	1,023759			
	1,04583	1,044066	Line 7	1,044852	1,076067	1,045519			
	1,044914	1,045535		1,040545	1,056993	1,048649			
	1,043182	1,041841		1,043198	1,049052	1,040055			
	1,042382	1,051499		1,039445	1,050501	1,040619			
	1,051397	1,048031	Line 8	1,039956	1,06294	1,046468			
	1,046738	1,048206		1,035979	1,051756	1,045479			
	1,039363	1,045535		1,03836	1,045164	1,034716			
	1,043962	1,04163		1,028186	1,039638	1,024558			
	1,045431	1,044323	Line 9	1,039894	1,059585	1,049332			
	1,044321	1,043621		1,031407	1,045592	1,04615			
	1,048745	1,044272		1,036991	1,043165	1,042214			
	1,046507	1,040226		1,032043	1,0488	1,039845			
	1,046776	1,04638	Line 10	1,038949	1,059763	1,043101			
	1,045616	1,04557		1,031621	1,060716	1,048726			
	1,043677	1,040711		1,023762	1,047278	1,042054			
	1,040499	1,048572		1,036286	1,056917	1,040714			
	1,047346	1,049881	Line 11	1,030611	1,05375	1,045846			
	1,048833	1,048001		1,039348	1,040731	1,04078			
1,044072	1,042448	1,028246		1,05301	1,029491				
1,046687	1,045517	1,032883		1,058969	1,029422				
1,052465	1,053565	Line 12	1,025825	1,053907	1,040201				
1,048467	1,047704		1,027593	1,039384	1,03595				
1,049043	1,048433		1,022381	1,040702	1,031479				
1,051077	1,04601		1,030036	1,042495	1,019243				

**Table 6.4 Individual fitness values for all replicates of strain I2 and corresponding lines, across bottlenecks 0, 48 and 144. Blank cells represent replicates that could not be measured or were used as controls.**

	B0		B48				B144		
I2	1,063921	Line 1	1,039083	1,041588	1,034359	Line 1	1,029618	1,039293	1,059272
	1,038553		1,046372	1,028222	1,032806	Line 2	0,997034	1,032297	1,040939
	1,047755		1,054166	1,043361	1,037481	Line 3	1,015702	1,029639	1,024307
			1,058586	1,042067	1,026841	Line 4	1,041798	1,050216	1,014554
	1,078458	Line 2		1,019546		Line 5	1,036345	1,057287	1,048103
	1,062112		1,043455	1,014017	1,031599	Line 6	1,028037	1,027704	1,041031
	1,095842		1,048042	1,035734	1,017264	Line 7	1,024578	1,035044	1,031415
	1,082199		1,049286	1,017893	1,011974	Line 8	0,929844	0,918095	0,929678
	1,071695	Line 3	1,046568	1,06017	1,030079	Line 9	1,033757	1,015633	1,028022
	1,046536				1,047053	Line 10	0,991679	1,001332	1,012675
	1,072844		1,047959	1,039527	1,027709	Line 11	0,88119	0,869414	0,874628
	1,074645		1,055415	1,061591	1,032536	Line 12	0,978015	0,966235	0,983857
	1,071253	Line 4	1,010323	1,043129	1,033291				
	1,062261		1,014869	1,032513	1,020643				
	1,046083								
	1,081652		1,036361	1,041642	1,031288				
	1,050239	Line 5	1,025928	1,034172	1,026147				
	1,056051		1,038387	1,041638	1,015382				
	1,076263		1,048208	1,027048	1,034736				
	1,04395		1,039755						
	1,066925	Line 6	1,068279	1,042902	1,024069				
	1,075196		1,07555	1,036033	1,026204				
	1,072436		1,075228	1,032609	1,015624				
	1,05933		1,088248	1,048263	1,01427				
	1,067487	Line 7	1,046367	1,017108	1,016732				
	1,072508		1,048104	1,034548	1,01421				
	1,050912		1,046678	1,020665	1,012817				
	1,071351		1,059509	1,047239	0,99988				
	1,047626	Line 8	1,091969	1,038649	1,039185				
	1,042146		1,073316	1,014588	1,031727				
	1,061019		1,097997	1,026253	1,0284				
			1,094284	1,039614	1,025458				
	1,062393	Line 9	1,094546	1,036896	1,02878				
	1,05221		1,100255	1,016367	1,028362				
	1,06687		1,072943	1,058702	1,022728				
	1,048665		1,086562	1,019985	1,015168				
		Line 10	1,063652	1,020634	1,019659				
			1,066091	1,020559	1,036034				
			1,079282	1,030131	1,016201				
			1,097108	1,046417	1,020943				
	Line 11	1,1087	1,031511	1,02366					
		1,108697	1,02204	1,037599					
		1,096784	0,989359	1,026652					
		1,089899	0,991509	1,028326					
	Line 12	1,060859	1,055839	1,023615					
		1,083741	1,038169	1,03863					
		1,054386	1,034051	1,020762					
		1,060805	1,037117	1,016698					



**Table 6.5 Individual fitness values for all replicates of strain C2 and corresponding lines, across bottlenecks 0, 48 and 144. Blank cells represent replicates that could not be measured or were used as controls.**

	B0			B48				B144		
C2	1,018087	Line 1	1,050089	1,054748	1,033188	Line 1	1,002366	0,928007	1,032459	
	1,014009		1,049162	1,054484	1,026578	Line 2	1,018641	1,01298	0,987696	
	1,022765		1,049286	1,048204	1,027401	Line 3	1,049968	1,148652	1,075681	
			1,044498	1,076196	1,027456	Line 4	0,89338	0,881942	0,84788	
	1,012989	Line 2		1,088904		Line 5	1,04363	1,068281	1,042133	
	1,030922		1,066251	1,076477	1,052131	Line 6		1,045607	1,055545	
	1,035775		1,070121	1,066298	1,045966	Line 7	0,99785	1,027007	0,989563	
	1,029814		1,073339	1,057	1,041551	Line 8	1,043926	1,07333	1,052639	
	1,027211	Line 3	1,073136	1,067322	1,048923	Line 9	1,040356	1,047123	1,027141	
	1,018893				1,0444	Line 10	1,036808	1,035629	1,032307	
	1,016074		1,073154	1,073063	1,040689	Line 11	1,0646	1,085291	1,06085	
	1,033319		1,08845	1,085802	1,047527	Line 12	extinct			
	1,018653	Line 4	1,095714	1,0793	1,053923					
	1,021072		1,081494	1,081613	1,041006					
	1,025067									
	1,026172		1,083292	1,064747	1,041381					
	1,020457	Line 5	1,079823	1,065357	1,045535					
	1,018958		1,062919	1,080201	1,039364					
			1,081232	1,073735	1,045263					
	1,0292		1,078338							
	1,011719	Line 6	1,079787	1,070198	1,037823					
	1,019707		1,065594	1,052543	1,032031					
	1,040259		1,07019	1,067675	1,030039					
	1,017196		1,074085	1,071348	1,022794					
	1,046764	Line 7	1,097985	1,0288	1,001745					
	1,014205		1,05886	1,017784	0,992105					
	1,043371		1,030351	1,024481	0,998713					
	1,032136		1,037862	1,030534	0,993893					
	1,034204	Line 8	1,112278	1,072565	1,048485					
	1,039161		1,067006	1,084049	1,042223					
	1,036372		1,082622	1,083988	1,036548					
	1,017472		1,08464	1,08065	1,044239					
		Line 9	1,077994	1,081653	1,050749					
	1,01248		1,084526	1,087851	1,038355					
	1,03035		1,072879	1,067184	1,036012					
	1,036588		1,074398	1,077975	1,037849					
		Line 10	1,027755	1,046823	1,011442					
			1,002985	1,084442	1,006391					
			1,04335	1,048459	1,015572					
			1,005281	1,059668	1,00048					
	Line 11	1,061567	1,078477	1,037198						
		1,062874	1,093017	1,042521						
		1,06693	1,078645	1,040166						
		1,061985	1,076207	1,04906						
	Line 12	0,993549	1,019289	0,982384						
		1,00357	1,013089	0,974277						
		0,994567	1,002294	0,96399						
		1,007225	0,988596	0,968708						

**Table 6.6 Individual fitness values for all replicates of strain T4 and corresponding lines, across bottlenecks 0, 48 and 144. Blank cells represent replicates that could not be measured or were used as controls.**

	B0		B48					B144	
T4	0,865094	Line 1	0,953908	0,898717	0,908617	0,885093	Line 1	1,040441	1,039363
	0,844044		0,955067	0,906956	0,90741	0,886638	Line 2	1,024381	1,035068
	0,86796		0,940333	0,886989	0,901769	0,887135	Line 3	1,007394	0,988959
	0,859862		0,953836	0,884124	0,909255	0,886264	Line 4	1,031977	1,01369
	0,871855	Line 2					Line 5	1,037491	1,055104
	0,828085		0,918282	0,905084	0,903645	0,89322	Line 6	1,008833	0,989745
	0,830566		0,931554	0,920996	0,917752	0,893324	Line 7	1,037472	1,043099
	0,822229		0,922535	0,89213	0,907348	0,884263	Line 8	1,029719	1,03683
	0,872488	Line 3	0,963714	0,900094	0,922929	0,898504	Line 9	1,045198	1,03905
	0,880583						Line 10	1,020532	1,04098
	0,86959		1,031099	0,899227	0,909178	0,896819	Line 11	1,021544	1,021838
	0,869492		0,972674	0,886351	0,907139	0,897693	Line 12	0,989339	0,985215
	0,90938	Line 4	0,911501	0,912538	0,898377	0,890881			
	0,870813		0,93865	0,89813	0,914887	0,89181			
	0,891192								
			0,979679	0,901761	0,908361	0,897874			
	0,856572	Line 5	0,924964	0,883712	0,88812	0,868593			
	0,865097		0,989067	0,873514	0,873732	0,878951			
	0,894247		0,930436	0,879952	0,886242	0,883589			
	0,867898								
	0,868735	Line 6	0,945473	0,89979	0,911191	0,895244			
	0,883875		0,96503	0,894896	0,908729	0,885908			
	0,864055		0,983155	0,897445	0,910434	0,912093			
	0,893559		0,987477	0,893284	0,90818	0,877864			
	0,916421	Line 7	0,945348	0,910239	0,912852	0,894681			
	0,907368		0,970473	0,907594	0,908169	0,895267			
	0,905767		0,949537	0,908594	0,900929	0,917089			
	0,87435		0,943109	0,889716	0,91443	0,897623			
	0,896431	Line 8	0,947688	0,914965	0,899628	0,89892			
	0,874656		1,107936	0,891847	0,900898	0,885764			
	0,896933		0,98446	0,90591	0,896981	0,886611			
	0,897749		0,986779	0,897707	0,910753	0,891854			
	0,884316	Line 9	0,96079	0,90986	0,904962	0,898544			
	0,883561		0,951119	0,90386	0,91108	0,879091			
	0,881525		0,968745	0,908032	0,897285	0,891353			
	0,877768		0,973158	0,892682	0,899847	0,889679			
		Line 10	0,949562	0,904043	0,891974	0,896238			
			0,898067	0,898153	0,919251	0,8937			
			0,943349	0,892545	0,907877	0,886824			
			0,958084	0,903023	0,903321	0,888718			
	Line 11	0,926933	0,903504	0,902059	0,906053				
		0,965622	0,908866	0,897821	0,910529				
		0,936897	0,915948	0,912401	0,893949				
		0,935459	0,89638	0,901964	0,902365				
	Line 12	0,94506	0,905312	0,901845	0,896099				
		0,940486	0,907125	0,905901	0,886705				
		0,920059	0,912812	0,884507	0,884289				
		0,958722	0,902468	0,897351	0,893214				

**Table 6.7 Individual fitness values for all replicates of strain C4 and corresponding lines, across bottlenecks 0, 48 and 144. Blank cells represent replicates that could not be measured or were used as controls.**

	B0		B48					B144	
C4	0,982415	Line 1	0,994913	0,990429	0,998635	1,003609	Line 1	0,972886	0,977172
	0,992326		0,988556	0,997672	1,000302	1,003718	Line 2	0,969169	0,959706
			0,986496	0,996325	0,999467	1,007035	Line 3	0,969771	0,964072
	0,990896	Line 2	0,991901	0,98226	0,998142	1,000068	Line 4	0,960918	0,957686
	0,991775		0,959001	0,965304	0,962712	0,967766	Line 5	0,999679	0,995363
	0,991192		0,96666	0,965299	0,966262	0,968011	Line 6	0,989679	0,947441
	0,993575	Line 3	0,957887	0,962038	0,964532	0,965003	Line 7	0,954852	0,949551
	0,992616		0,968709	0,96349	0,968028	0,96759	Line 8	0,971983	0,96791
	0,98468		0,982562	0,983989	0,991352	0,984625	Line 9	0,986598	0,993648
	0,991315	Line 4	0,970015	0,977092	0,983128	0,987404	Line 10	0,991106	0,983048
	0,99454		0,965088	0,982569	0,981124	0,97902	Line 11	0,954323	0,961923
	0,994159		0,970787	0,985728	0,979334	0,981328	Line 12	0,993812	0,986002
	0,987257	Line 5	0,983429	0,987001	0,988052	0,986029			
	0,98563			0,995377	0,979804	0,986183			
	0,989074		0,978362	0,995531	0,988009	0,986683			
	0,992066	Line 6	0,989652	0,994258	0,986325	0,989859			
			0,988905	0,992392	0,994828	0,997303			
				0,994007	0,993319	0,992879			
	0,991271	Line 7	0,986328	0,992946	0,988336	1,000791			
	0,99493		0,989812	0,986782	0,984989	0,994678			
	0,992614								
	0,99362	Line 8							
	0,991796		0,98487	0,990836	0,992529	1,000329			
	0,990979		0,994756	0,995345	0,996674	0,999555			
	0,993402	Line 9	0,99247	0,995106	0,980323	0,999249			
	0,996349		0,988419	0,988402	0,991078	0,996034			
	0,989844								
	0,997238	Line 10	0,986208	0,992997	0,991567	0,993893			
	0,994859		0,990781	0,991101	0,990727	0,996575			
	0,991759		0,995307	0,995049	0,992548	0,99404			
	0,99361	Line 11	0,985442	0,992551	0,990911	0,997881			
	0,990907	Line 12	0,99456	0,98768	0,990974	0,985586			
	0,989736		0,990602	0,989624	0,989871	0,995642			
	0,991607		0,98568	0,978722	0,983501	0,98715			
	0,996436	Line 13	0,98175	0,980138	0,984289	0,994703			
	0,987964								
		Line 14	0,98763	0,985706	0,990532	0,985968			
	0,987447		0,973703	0,98474	0,982312				
	0,98909		0,968384	0,98895	0,989579				
	Line 15	0,991732	0,986039	0,986946	0,990508				
		0,991463	0,962959	0,956268	0,889627				
		0,954796	0,963652	0,954611	0,938806				
	Line 16	0,99733	0,963952	0,953091	0,931852				
		0,960126	0,960269	0,956743	0,917108				
		0,965555	0,985704	0,986756	0,993693				
	Line 17	0,984339	0,987022	0,989666	0,99388				
		0,968055	0,981289	0,98464	0,986542				
		0,993873	0,993936	0,983033	0,991943				

**Table 6.8 Individual fitness values for all replicates of strain T5 and corresponding lines, across bottlenecks 0, 48 and 144. Blank cells represent replicates that could not be measured or were used as controls.**

	B0		B48				B144		
T5	0,916944	Line 1	0,933769	0,88152	0,921577	Line 1	0,816479	0,848885	0,844821
	0,876687		0,915355	0,784186	0,88952	Line 2	0,741614	0,80781	0,808399
	0,863914		0,915884	0,907021	0,877906	Line 3	0,78167	0,814564	0,844888
	0,884146		0,914516	0,801153	0,885643	Line 4	0,723837		0,735796
	0,858977	Line 2	0,865607	0,893614	0,860467	Line 5	0,790206	0,825634	0,802961
	0,860459		0,878552	0,809356	0,869744	Line 6	0,792012	0,823488	0,848742
	0,849009		0,892222	0,820037	0,866658	Line 7	0,760474		0,805838
	0,883106		0,826984	0,824634	0,859394	Line 8	0,803261	0,781391	0,792486
	0,902421	Line 3	0,868568	0,872841	0,887104	Line 9	0,769037	0,833574	0,840171
	0,864192		0,860516	0,770885	0,872491	Line 10	0,832455	0,845833	0,849771
	0,877274		0,892539	0,811649	0,870508	Line 11	0,802395	0,859009	0,853856
	0,897595		0,883283	0,8045	0,863477	Line 12	0,869745	0,854922	0,829784
	0,876245	Line 4	0,756128	0,691145	0,808798				
	0,852446		0,737281	0,755421	0,78676				
	0,903288		0,813205		0,800101				
	0,893738		0,778548	0,72291	0,835843				
	0,87271	Line 5	0,908928	0,858997	0,853388				
	0,886777		0,913411	0,939983	0,872783				
	0,877709		0,89926	0,928805	0,85169				
			0,897496	0,921627	0,855161				
	0,885489	Line 6		0,852131	0,868422				
	0,889069		0,89779	0,891503	0,87513				
	0,908185		0,905068	0,833823	0,86486				
	0,868149		0,912778	0,88552	0,873627				
	0,913222	Line 7	0,914364	0,907293	0,977306				
	0,893711				0,84405				
	0,8952		0,916226	0,892389	0,865725				
	0,892039		0,918747	0,823951	0,873456				
	0,894778	Line 8	0,898759	0,912363	0,875357				
	0,88513		0,890089	0,824269	0,859791				
	0,905804								
	0,90979		0,900363	0,845111	0,792556				
	0,880992	Line 9	0,90264	0,910853	0,88694				
	0,904336		0,894212	0,901242	0,867934				
	0,901194		0,926452	0,832819	0,882043				
	0,887433		0,882755						
		Line 10	0,904558	0,874771	0,870506				
			0,904049	0,94238	0,857703				
			0,915951	0,796614	0,852594				
			0,885196	0,823083	0,799072				
		Line 11	0,917622	0,828187	0,936452				
			0,908055	0,787772	0,928889				
	0,905114		0,841216	0,933181					
	0,917772		0,816135	0,932395					
	Line 12	0,898621	0,921549	0,85741					
		0,902701	0,804897	0,859722					
		0,905623	0,788278	0,844624					
		0,903909	0,809376	0,84899					

**Table 6.9 Individual fitness values for all replicates of strain C5 and corresponding lines, across bottlenecks 0, 48 and 144. Blank cells represent replicates that could not be measured or were used as controls.**

	B0		B48				B144		
C5	1,065773	Line 1	1,068676	1,048829	1,030218	Line 1	1,04014	1,057105	1,044208
	1,042561		1,043175	1,068529	1,035014	Line 2	1,005528	1,023046	1,035832
	1,063182		1,064491	1,062743	1,031154	Line 3	0,979547	0,992443	0,981222
	1,065444		1,064442	1,057195	1,038009	Line 4	1,027567	1,067059	1,025138
	1,053419	Line 2	1,006334	1,029423		Line 5	0,690717	0,733685	0,760882
	1,050296		1,006952	1,035792	0,981132	Line 6	1,033988	1,057405	1,035389
			1,072523	1,008422	0,992674	Line 7	1,033895	1,046679	1,048353
	1,061527		1,045073	1,014724	0,988073	Line 8	1,034684	1,05343	1,054375
	1,049011	Line 3	1,021485	1,05005	1,014155	Line 9	0,972782	0,969824	0,950444
	1,054149		1,051883	1,043339	1,013046	Line 10	0,996303	0,973092	1,019357
	1,065832		1,036641	1,045369	0,998488	Line 11	1,023721	1,046399	1,006778
	1,072351		1,034516	1,033994	1,01467	Line 12	1,000761	1,008065	0,994489
	1,057992	Line 4	1,091119	1,064774	1,03148				
	1,057356		1,095634	1,070269	1,035297				
	1,06018		1,080074	1,064217					
	1,075418		1,094413	1,064173	1,032801				
	1,064747	Line 5	1,067299	1,064726	1,028608				
	1,06162		1,075357	1,063016	1,035397				
	1,071059		1,051451	1,05697	1,035027				
	1,057949		1,076112	1,05875					
		Line 6		1,062749	1,018194				
	1,048634		1,041023	1,047145	1,020419				
	1,060515		1,048377	1,053738	1,0234				
	1,06914		1,038585	1,05415	1,032797				
	1,04954	Line 7	1,06314	1,065826	1,030862				
	1,047				1,031739				
			1,050166	1,056392	1,033335				
	1,039571		1,056298	1,068176	1,037148				
	1,042581	Line 8	1,069431	1,073444	1,035297				
	1,048086		1,067054	1,079999	1,033805				
	1,051809				1,026298				
	1,058081		1,057458	1,070085	1,029257				
	1,05197	Line 9	1,048614	1,059487	1,023791				
	1,053401		1,061565	1,057946	1,031306				
	1,046076		1,062356	1,051907	1,030465				
	1,053915		1,055598		1,037287				
		Line 10	1,06101	1,056181	1,029481				
			1,054016	1,062796	1,031095				
			1,058537	1,05169	1,031555				
			1,036613	1,050735	1,034687				
	Line 11	1,054214	1,060605	1,040444					
		1,070788	1,073938	1,039624					
		1,057144	1,059885	1,036042					
		1,071931	1,061731	1,044643					
	Line 12	1,079618	1,052376	1,039623					
		1,07242	1,067211	1,041819					
		1,082792	1,062198	1,035487					
		1,064323	1,056783	1,045522					

**Table 6.10 Individual fitness values for all replicates of strain SPP20 and corresponding lines, across bottlenecks 0, 48 and 144. Blank cells represent replicates that could not be measured or were used as controls.**

	B0			B48		
SPP20	0,999768		Line 1	1,030463	1,035174	1,027604
	1,017488		Line 2	1,025195	1,046489	1,039394
	1,021328		Line 3	1,024502	1,038184	1,011796
	0,993171		Line 4	1,029193		1,013392
	0,988256		Line 5	1,034851	1,019368	1,024542
	0,999964		Line 6	1,029076	1,019673	1,008276
	1,020007		Line 7	1,037457	1,034958	1,00813
	1,013695		Line 8	1,030552	1,034051	1,023122
	1,027592		Line 9	1,035473	1,027433	0,985634
	1,020075		Line 10	1,03856	1,05727	1,022383
	1,007081		Line 11	1,032417	1,047048	1,020197
	1,023908		Line 12	1,028209		1,015447
	1,025181					
	1,018394					
	1,019051					
	1,021722					
	1,019339					
	1,026682					

**Table 6.11 Individual fitness values for all replicates of strain T8 and corresponding lines, across bottlenecks 0, 48 and 144. Blank cells represent replicates that could not be measured or were used as controls.**

	B0		B48						B144		
T8	0,923249	Line 1	0,885862	0,880377	0,879372	0,864105	Line 1	0,835874	0,854694	0,839691	
	0,887685		0,885176	0,874607	0,855284	0,857127	Line 2	0,826886	0,823157	0,800183	
	0,852831		0,865647	0,877291	0,876346	0,861384	Line 3	0,81157	0,846828	0,84227	
	0,854828		0,892621	0,86628	0,863091	0,863034	Line 4	0,850898	0,867141	0,787863	
	0,882154	Line 2			0,871973		Line 5	0,763896	0,810427	0,781749	
	0,849276		0,888751	0,874753	0,859976	0,853231	Line 6	0,845714	0,814374	0,844935	
	0,868831		0,883571	0,883283	0,867	0,858068	Line 7	0,818705	0,816155	0,802419	
	0,874066		0,891323	0,873198	0,88118	0,853155	Line 8	0,804917	0,829216	0,832422	
		Line 3	0,886608	0,875883	0,890183	0,895467	Line 9	0,823958	0,82348	0,823198	
	0,849318					0,885991	Line 10	0,834132	0,813819	0,821625	
	0,851741		0,883614	0,888685	0,889061	0,875065	Line 11	0,733583	0,80596	0,771187	
	0,85098		0,860873	0,872142	0,887007	0,884205	Line 12	0,858814	0,859495	0,855441	
	0,911687	Line 4	0,888799	0,891744	0,885931	0,8985					
	0,880764		0,913239	0,908946	0,901939	0,894622					
			0,893611								
	0,844635	Line 5	0,902398	0,908543	0,893188	0,889924					
	0,894601		0,871385	0,883287	0,882358	0,893065					
	0,882994		0,890528	0,88574	0,888258	0,88395					
	0,860902		0,892926	0,905613	0,895612	0,886777					
	0,888041		0,883433								
	0,867488	Line 6	0,883109	0,888922	0,846596	0,863366					
	0,88442		0,896254	0,885151	0,888807	0,862448					
	0,860443		0,883268	0,88732	0,874821	0,885259					
	0,894832	Line 7	0,914222	0,882435	0,896866	0,860363					
	0,866149		0,878199	0,907786	0,892551	0,891655					
	0,847578		0,889615	0,909758	0,904819	0,900286					
	0,864981		0,893122	0,893261	0,902925	0,890338					
	0,859162		0,883727	0,889537	0,887012	0,887955					
		Line 8	0,87756	0,888763	0,87053	0,867226					
	0,84779		0,894872	0,905268	0,894484	0,876104					
	0,861325		0,903167	0,883398	0,889516	0,8736					
	0,850229		0,892288	0,89874	0,867799	0,894142					
	0,852138	Line 9	0,882442	0,893588	0,898523	0,888315					
	0,848576		0,897897	0,891004	0,899445	0,893208					
	0,861698		0,886018	0,880213	0,871456	0,8726					
	0,829412		0,884186	0,894171	0,887895	0,870403					
		Line 10	0,864612	0,893118	0,89014	0,876251					
			0,889588	0,872922	0,886871	0,871178					
			0,914369	0,881978	0,884663	0,876186					
		Line 11	0,882435	0,894815	0,859707	0,868932					
			0,884953	0,870543	0,902779	0,871045					
			0,885767	0,873646	0,876949	0,888913					
			0,901541	0,869586	0,865458	0,895945					
			0,892991	0,870046	0,8594	0,880982					
		Line 12	0,903694	0,889697	0,885019	0,887438					
			0,89521	0,882738	0,890729	0,868522					
			0,888456	0,892413	0,863645	0,899171					
			0,896194	0,876672	0,880484	0,864844					

**Table 6.12 Individual fitness values for all replicates of strain C8 and corresponding lines, across bottlenecks 0, 48 and 144. Blank cells represent replicates that could not be measured or were used as controls.**

	B0			B48				B144		
C8	0,984987	Line 1	0,990607	0,987884	0,974908	Line 1	0,979241	0,969764	0,976163	
	0,984679		0,97759	0,985845	0,9719	Line 2	0,905344		0,912032	
	0,981833		0,984931	0,985802	0,971691	Line 3	0,982698	0,97644	0,978592	
	0,987675		0,972523	0,985441	0,971534	Line 4	0,976926	0,97095	0,972885	
	0,983903	Line 2	0,975431	0,982838	0,968127	Line 5	0,975568	0,974164	0,977889	
	0,983606		0,980575	0,980049	0,963187	Line 6		0,951477	0,95489	
	0,985121		0,975519	0,974776	0,960158	Line 7	extinct			
			0,973781	0,974686	0,956261	Line 8				
	0,987864	Line 3	0,989009	0,991157	0,978851	Line 9	0,925551	0,927646	0,921827	
	0,982375		0,988886	0,991826	0,98269	Line 10	0,98021	0,977162	0,981227	
	0,985933		0,985582	0,990508	0,978514	Line 11	0,979134	0,982982	0,988082	
	0,982845		0,987542	0,98708	0,976634	Line 12	0,945884	0,93522	0,93859	
	0,983506	Line 4	0,983313	0,989222	0,976869					
	0,986002		0,986157	0,987275	0,971682					
	0,984046		0,984219	0,982986	0,96493					
	0,981382		0,982519	0,986473	0,970297					
	0,98164	Line 5	0,98726	0,989366	0,979274					
	0,982246		0,978533	0,990538	0,982374					
	0,986015		0,984439	0,985429	0,970432					
	0,979891		0,987961	0,987038	0,977522					
	0,983779	Line 6			0,976311					
	0,983043		0,986786	0,984991	0,974832					
	0,983323		0,977318	0,987593	0,972882					
	0,986327		0,981701	0,972529	0,967927					
	0,986664	Line 7	0,983912	0,988385	0,973717					
	0,986188									
	0,988954		0,98298	0,984718	0,974296					
			0,984677	0,984976	0,973655					
	0,98982	Line 8	0,980538	0,983287	0,965099					
	0,988847		0,980136	0,980162	0,967494					
	0,989246		0,976604							
	0,990098	Line 9	0,97853	0,979425	0,973561					
	0,988742		0,979212	0,981048	0,971679					
	0,988225		0,976824	0,982359	0,973424					
	0,98889		0,97988	0,979489	0,97395					
	0,989464			0,980568						
		Line 10	0,965003	0,96706	0,959873					
			0,963539	0,97093	0,957869					
			0,966724	0,961977	0,950435					
			0,960941	0,966231	0,948314					
	Line 11	0,975641	0,978252	0,967582						
		0,979132	0,979416	0,966448						
		0,973276	0,980647	0,966991						
		0,977422	0,981495	0,964505						
	Line 12	0,980521	0,984166	0,9796						
		0,982841	0,983974	0,976641						
		0,981485	0,979683	0,975335						
		0,976126	0,983394	0,974413						



**Table 6.13 Individual fitness values for all replicates of strain T10 and corresponding lines, across bottlenecks 0, 48 and 144. Blank cells represent replicates that could not be measured or were used as controls.**

	B0			B48				B144		
T10	1,029278	Line 1		0,990056	0,994436	0,975359	Line 1	0,963352	0,960897	0,960903
	1,019201			0,976565	0,993583	0,971698	Line 2	0,9639	0,978828	0,97797
				0,975983	0,983047	0,977849	Line 3	1,003218	1,01062	1,009202
	1,018239			0,978735	0,983136	0,967545	Line 4	1,005306	1,026453	1,014985
	1,020206	Line 2				1,017858	Line 5	0,919191	0,874274	0,93583
	1,032017			1,020306	1,015483	1,02699	Line 6	0,955836	0,968918	0,955683
	1,015218			1,02271	1,015349	1,015886	Line 7	0,99951	1,009961	0,999748
	1,03452			1,01266	1,011168	1,024564	Line 8	0,933845	0,941471	0,964958
	1,025115	Line 3		1,018674	1,008078	1,018705	Line 9	1,019952	1,008095	1,024931
	1,027304						Line 10	1,002196	0,989797	0,992472
	1,034554			1,010464	1,012304	1,017633	Line 11	1,012194	1,002455	1,012158
	1,025994			1,016839	1,007856	1,017459	Line 12	1,004592	1,015368	1,017838
	1,006253	Line 4		1,019983	1,005928	1,021643				
	1,012032			1,017605	1,013841	1,020109				
	1,023765			1,018673						
	1,024909			1,014919	1,017291	1,016008				
		Line 5		1,018732	1,015253	1,019143				
	1,023696			1,014406	1,006817	1,018163				
	1,01519			1,012991	1,011726	1,015575				
	1,014701				1,014695					
	1,009232	Line 6		1,017469	1,007247	1,022282				
	1,011571			1,019257	1,006487	1,020965				
	1,02249			1,021434	1,007389	1,012951				
	1,016026			1,012876	1,013269	1,015632				
	1,006293	Line 7		1,014388	1,01943	1,010687				
	1,016744			1,011714	1,018155	1,020193				
	1,018905			1,009265	1,002654	1,018115				
	1,01459			1,009558	1,014857	1,011218				
	1,014756	Line 8		1,025747	1,023583	1,023458				
	1,00379			1,024626	1,020854	1,028158				
	1,012045			1,02498	1,03018	1,026452				
	1,010243			1,025058	1,024775	1,026698				
	1,010678	Line 9		1,020184	1,004798	1,017986				
	1,019991			1,012173	1,010438	1,022668				
	1,018008			1,011577	1,010398	1,015878				
	1,015065			1,013634	1,015402	1,01607				
		Line 10		1,009389	1,011297	1,010909				
				1,010563	1,010411	1,014737				
				1,009249	1,001714	1,00144				
				1,01254	1,013937	1,00868				
	Line 11		1,013038	1,008527	1,02112					
			1,021838	1,009502	1,010325					
			1,013842	1,013778	1,000088					
			1,012267	1,007745	1,009497					
	Line 12		1,014753	1,012568	1,013325					
			1,012684	1,011126	1,016291					
			1,018322	1,001367	1,017597					
			1,012415	1,010071	1,013325					

**Table 6.14 Individual fitness values for all replicates of strain C10 and corresponding lines, across bottlenecks 0, 48 and 144. Blank cells represent replicates that could not be measured or were used as controls.**

	B0		B48				B144		
C10	0,989018	Line 1	0,996785	0,992963	0,982874	Line 1	0,990558	0,987429	0,990664
	0,989216		0,997132	0,992222	0,985841	Line 2	0,926075		0,916246
	0,988406		0,996516	0,9871	0,991315	Line 3	0,982755		0,988503
	0,990556		0,998406	0,9889	0,991733	Line 4	0,981046	0,979112	0,980363
	0,985358	Line 2	0,998754	0,994249	0,994738	Line 5	0,961767	0,957702	0,96564
	0,98549		0,998903	0,988401	0,991436	Line 6		0,983473	0,980347
	0,988615		0,999825	0,997159	0,997634	Line 7	0,980116	0,983419	0,973416
	0,99203		1,000662	0,992872	0,997146	Line 8	0,954222	0,94286	0,95302
	0,985567	Line 3	0,979414	0,991035	0,987308	Line 9	0,988041	0,983064	0,988986
	0,987679		0,992146	1,027734	0,996213	Line 10	0,964189	0,965528	0,960434
	0,989225		0,991635	0,991704	0,995757	Line 11	0,980228	0,973571	0,968515
	0,999167		0,991017	0,992069	0,992774	Line 12	0,981537	0,983024	0,97932
	1,00445	Line 4	0,986387	0,99406	0,982193				
	1,001346		0,991543	0,98918	0,984549				
	1,000751		0,989827	0,984513	0,981069				
			0,992552	0,993963	0,992338				
	1,001103	Line 5	0,988283	0,983424	0,974143				
	1,001268		0,990792	0,992238	0,982212				
	1,000034		0,992069	0,985071	0,984826				
	1,003166		0,987863	0,991543	0,989966				
	0,999627	Line 6			0,972519				
	0,988241		0,972841	0,971414	0,966084				
	0,998494		0,975678	0,968843	0,971851				
	0,998386		0,972711	0,970306	0,982277				
	0,997257	Line 7	0,984753	0,981759	0,977755				
	0,995171								
	0,994139		0,984925	0,975076	0,983313				
	0,990284		0,985442	0,982003	0,97954				
	0,994639	Line 8	0,986352	0,989507	0,994246				
	0,996667		0,985282	0,980371	0,983479				
	0,994852		0,991816						
	0,990982	Line 9	0,980089	0,985209	0,989611				
	0,996215		0,988692	0,978866	0,991253				
	0,996373		0,986384	0,976567	0,98837				
	0,99394		0,992094	0,991722	0,994072				
	0,992267			0,981198					
		Line 10	0,979361	0,975075	0,979502				
			0,978601	0,969427	0,981952				
			0,986631	0,980066	0,979083				
			0,978874	0,980749	0,979264				
	Line 11	0,974485	0,97097	0,970694					
		0,974117	0,969104	0,969078					
		0,976476	0,979828	0,97059					
		0,978292	0,967139	0,978453					
	Line 12	0,983152	0,990583	0,971247					
		0,980997	0,977737	0,985355					
		0,979297	0,982422	0,982454					
		0,985783	0,9802	0,98241					

